

UHECRs cannot be protons from steady sources

necessary condition for successful particle acceleration

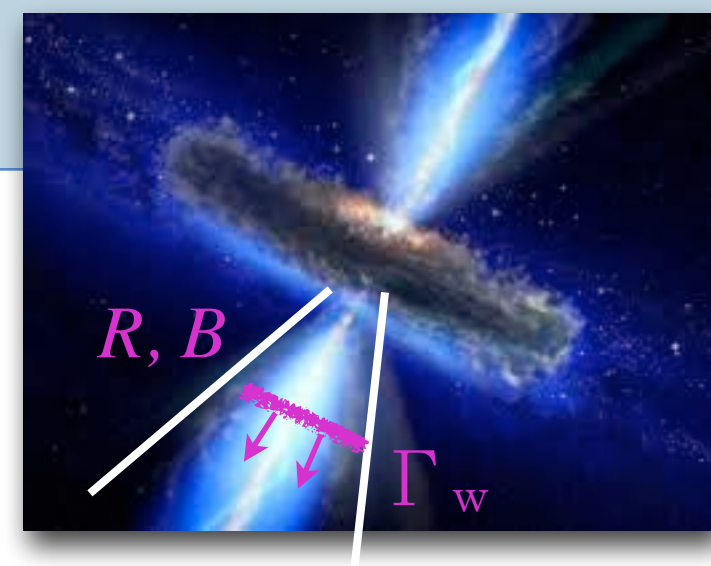
Lemoine & Waxman 09

$$\text{outflow magnetic luminosity } L_B \equiv \Gamma_W R^2 B^2 / 2 > 10^{45} Z^{-2} E_{20}^2 \text{ erg s}^{-1}$$

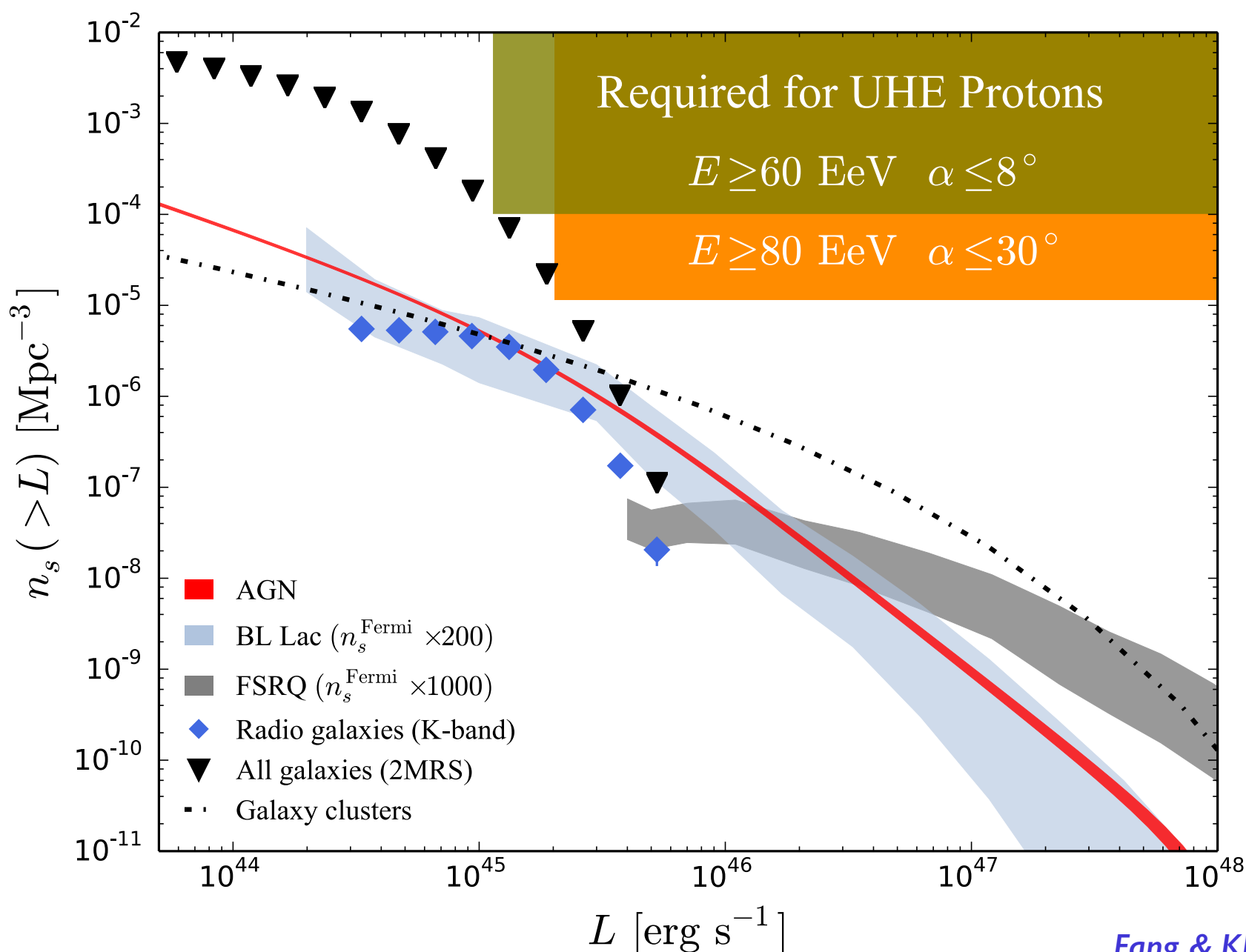
➤ lower bound of the bolometric luminosity of source

level of anisotropy in the sky in Auger data *Abreu et al. 2013*

➤ apparent number density of sources @ given energy and angular deflection α



Ke Fang's talk (Tuesday AM)



Fang & KK, submitted

The transient energy budget

level of anisotropy in the sky in Auger data

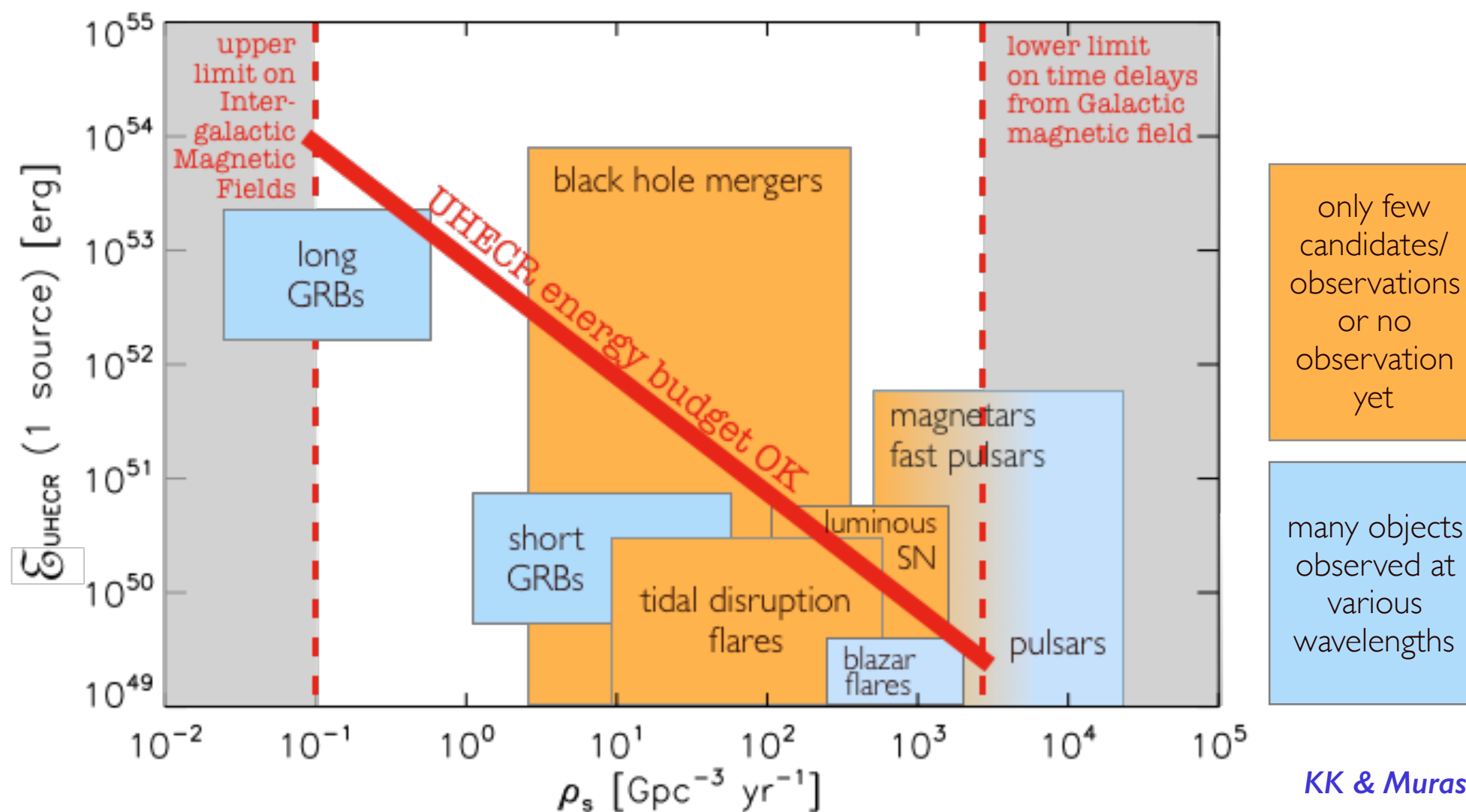
➤ **apparent number density of sources** n_0 @ given energy and angular deflection α

for transient sources: **real number density** of UHE proton sources

$$\rho_0 \sim n_0 / (\text{CR time spread } \tau_d)$$

τ_d depends on extragalactic + Galactic magnetic fields (not known) *Murase & Takami 09*

➤ Observed energy budget in UHECRs $E_{\text{UHECR}} \rho_0 = 10^{44.5} \text{ erg Mpc}^{-3} \text{ yr}^{-1}$



KK & Murase, in prep.

The transient energy budget

level of anisotropy in the sky in Auger data

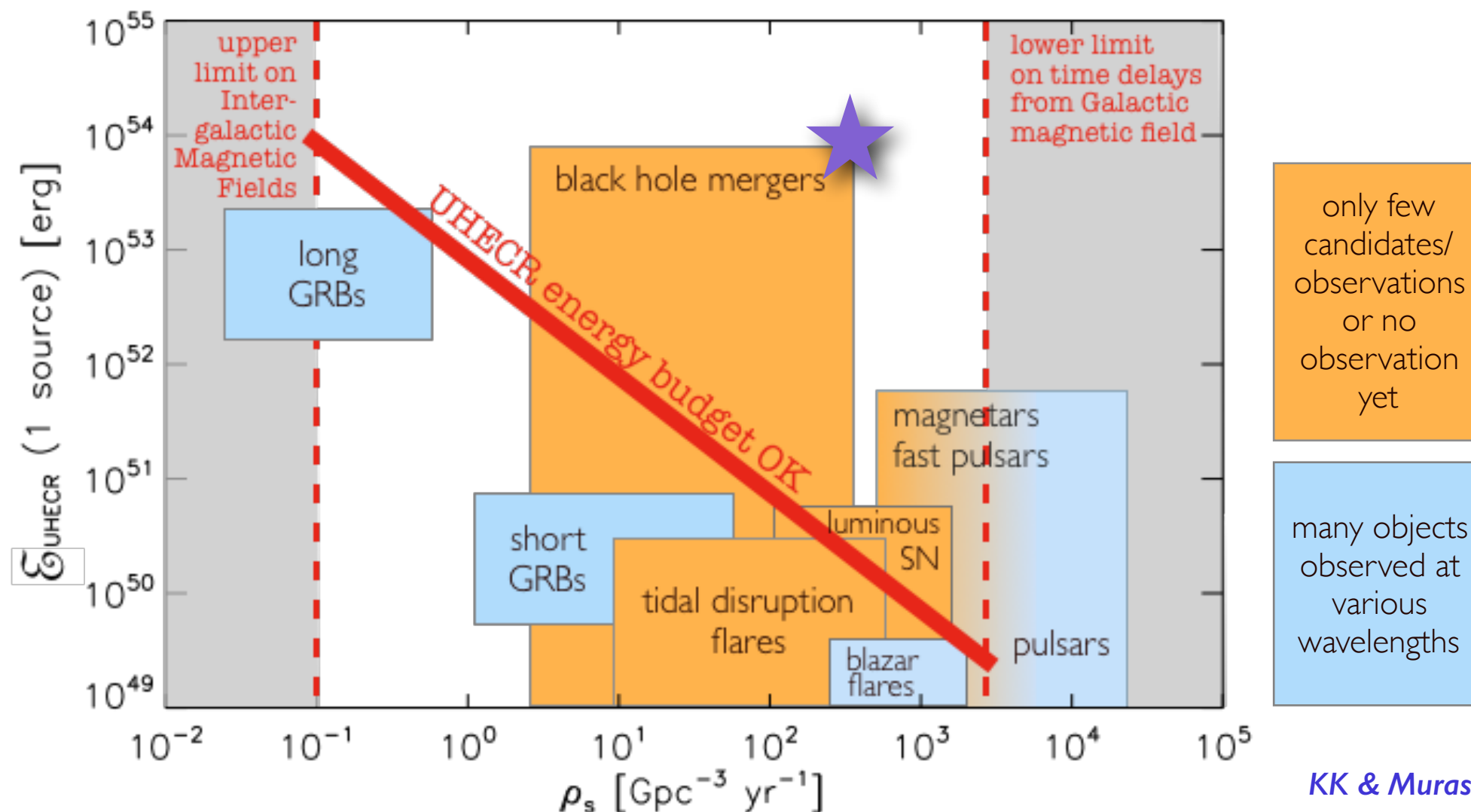
➤ **apparent number density of sources** n_0 @ given energy and angular deflection α

for transient sources: **real number density** of UHE proton sources

$$\rho_0 \sim n_0 / (\text{CR time spread } \tau_d)$$

τ_d depends on extragalactic + Galactic magnetic fields (not known) *Murase & Takami 09*

➤ Observed energy budget in UHECRs $E_{\text{UHECR}} \rho_0 = 10^{44.5} \text{ erg Mpc}^{-3} \text{ yr}^{-1}$



The transient energy budget

level of anisotropy in the sky in Auger data

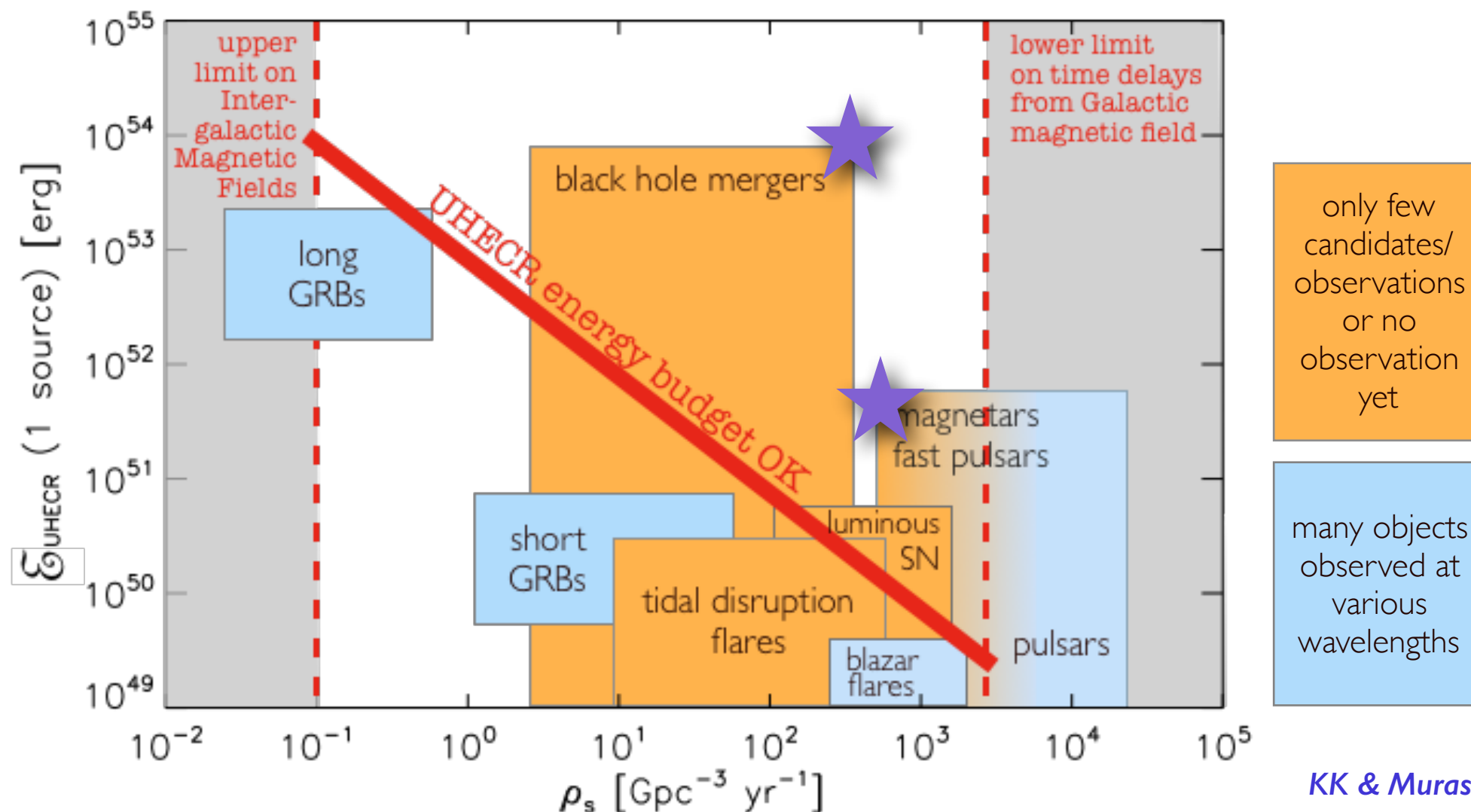
➤ **apparent number density of sources** n_0 @ given energy and angular deflection α

for transient sources: **real number density** of UHE proton sources

$$\rho_0 \sim n_0 / (\text{CR time spread } \tau_d)$$

τ_d depends on extragalactic + Galactic magnetic fields (not known) *Murase & Takami 09*

➤ Observed energy budget in UHECRs $E_{\text{UHECR}} \rho_0 = 10^{44.5} \text{ erg Mpc}^{-3} \text{ yr}^{-1}$



KK & Murase, in prep.

The transient energy budget

level of anisotropy in the sky in Auger data

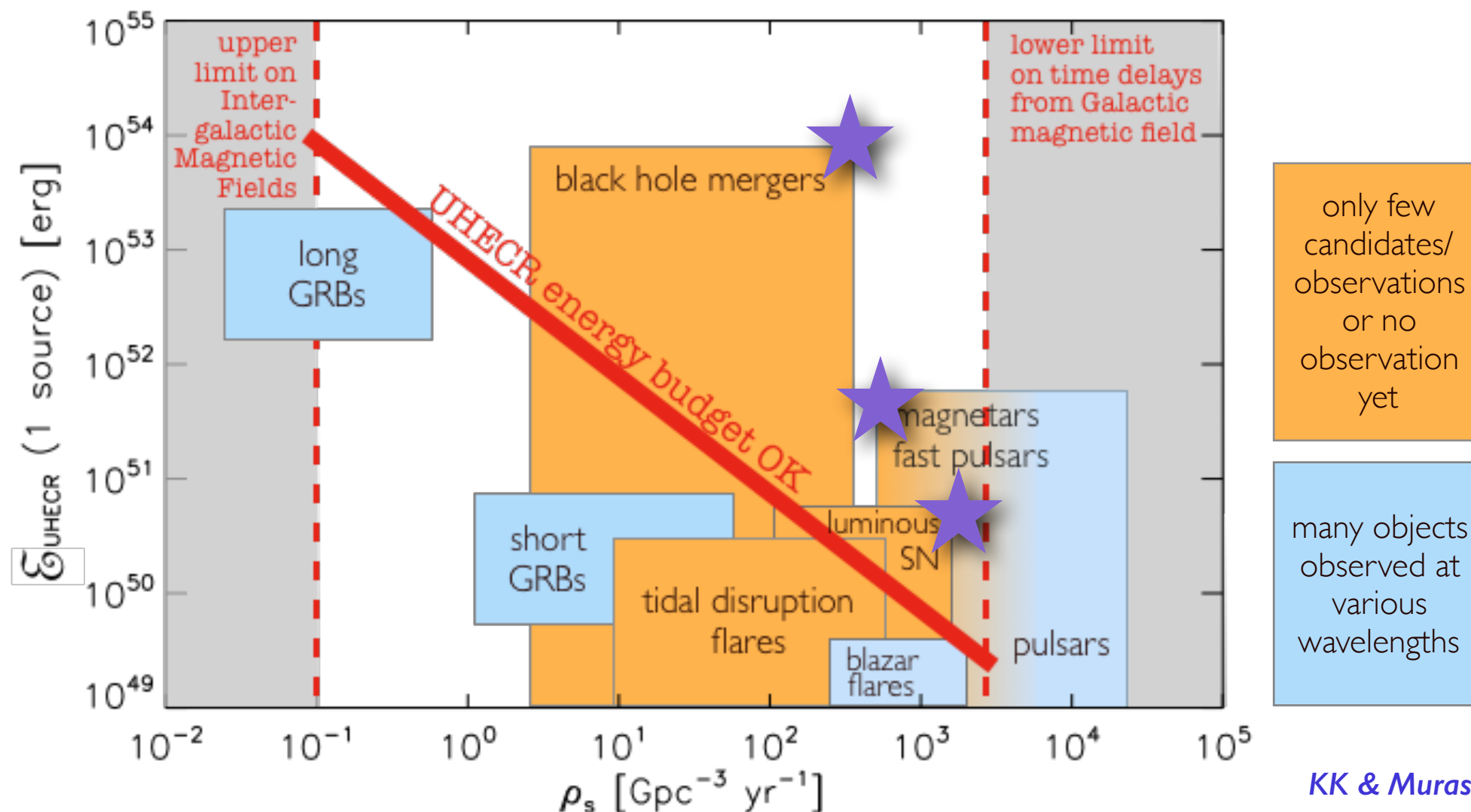
➤ **apparent number density of sources** n_0 @ given energy and angular deflection α

for transient sources: **real number density** of UHE proton sources

$$\rho_0 \sim n_0 / (\text{CR time spread } \tau_d)$$

τ_d depends on extragalactic + Galactic magnetic fields (not known) *Murase & Takami 09*

➤ Observed energy budget in UHECRs $E_{\text{UHECR}} \rho_0 = 10^{44.5} \text{ erg Mpc}^{-3} \text{ yr}^{-1}$



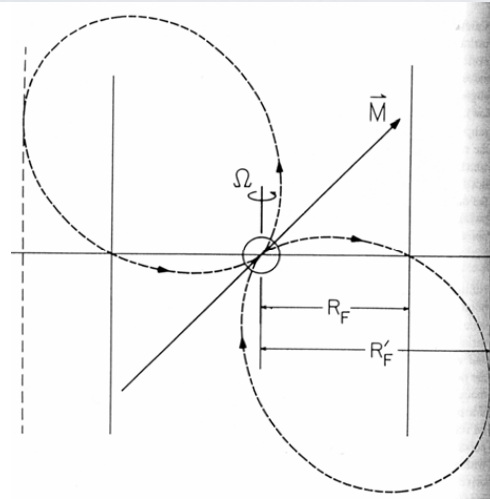
KK & Murase, in prep.

Particle acceleration in pulsars/magnetars

► Charge density

Induced electric field

$$\mathbf{E} = -\frac{\mathbf{v}}{c} \times \mathbf{B} = -\frac{1}{c}(\boldsymbol{\Omega} \times \mathbf{r}) \times \mathbf{B}$$



Implies a charge density (Goldreich-Julian 69)

$$\rho = \frac{1}{4\pi} \nabla \cdot \mathbf{E} \approx -\frac{\boldsymbol{\Omega} \cdot \mathbf{B}}{2\pi c} \equiv \rho_{GJ}$$

e.g.

Blasi et al. (2000)

Arons et al. (2003)

Bednarek & Bartosik (2006)

Fang, KK & Olinto (2012, 2013)

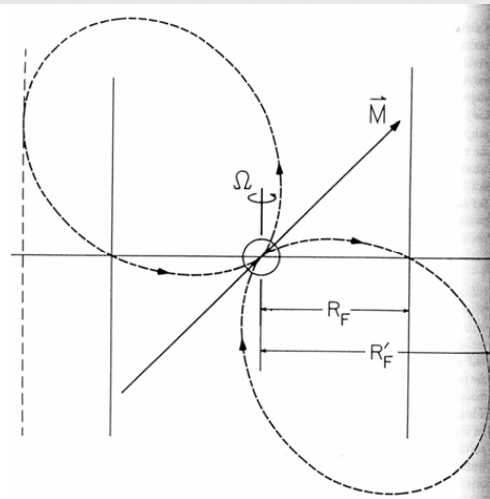
Lemoine, KK & Pétri (2015)

Particle acceleration in pulsars/magnetars

Charge density

Induced electric field

$$\mathbf{E} = -\frac{\mathbf{v}}{c} \times \mathbf{B} = -\frac{1}{c}(\boldsymbol{\Omega} \times \mathbf{r}) \times \mathbf{B}$$



Implies a charge density (Goldreich-Julian 69)

$$\rho = \frac{1}{4\pi} \nabla \cdot \mathbf{E} \approx -\frac{\boldsymbol{\Omega} \cdot \mathbf{B}}{2\pi c} \equiv \rho_{GJ}$$

e.g.

Blasi et al. (2000)

Arons et al. (2003)

Bednarek & Bartosik (2006)

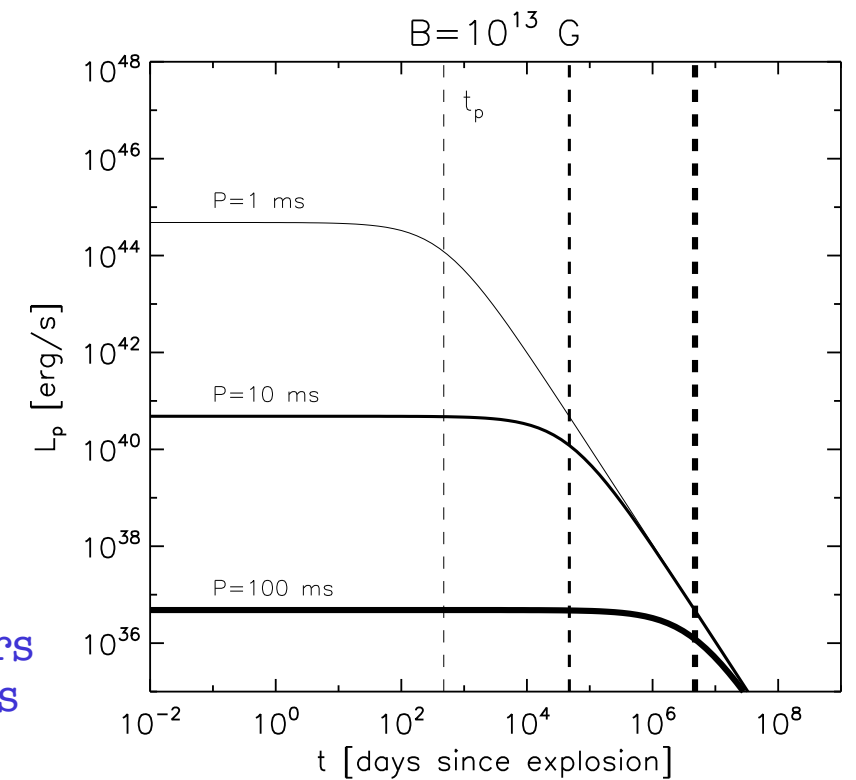
Fang, KK & Olinto (2012, 2013)

Lemoine, KK & Pétri (2015)

outflow energetics

total energy $E_p = \frac{I\Omega_i^2}{2} \sim 1.9 \times 10^{52} \text{ erg } I_{45} P_{i,-3}^2$

neutron star luminosity $L_p(t) = \frac{E_p}{t_p} \frac{1}{(1 + t/t_p)^2}$



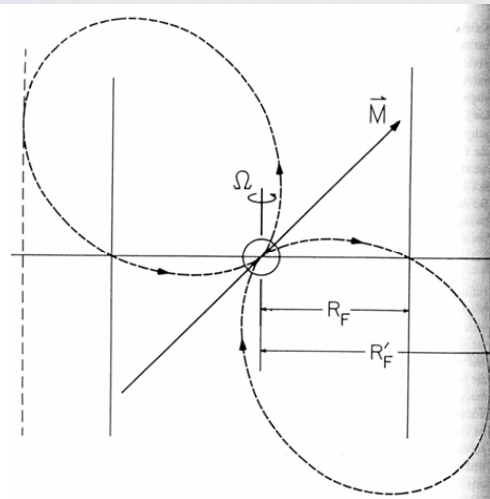
$t_p \sim$ a few years
for ms pulsars

Particle acceleration in pulsars/magnetars

Charge density

Induced electric field

$$\mathbf{E} = -\frac{\mathbf{v}}{c} \times \mathbf{B} = -\frac{1}{c}(\boldsymbol{\Omega} \times \mathbf{r}) \times \mathbf{B}$$



Implies a charge density (Goldreich-Julian 69)

$$\rho = \frac{1}{4\pi} \nabla \cdot \mathbf{E} \approx -\frac{\boldsymbol{\Omega} \cdot \mathbf{B}}{2\pi c} \equiv \rho_{GJ}$$

e.g.

Blasi et al. (2000)

Arons et al. (2003)

Bednarek & Bartosik (2006)

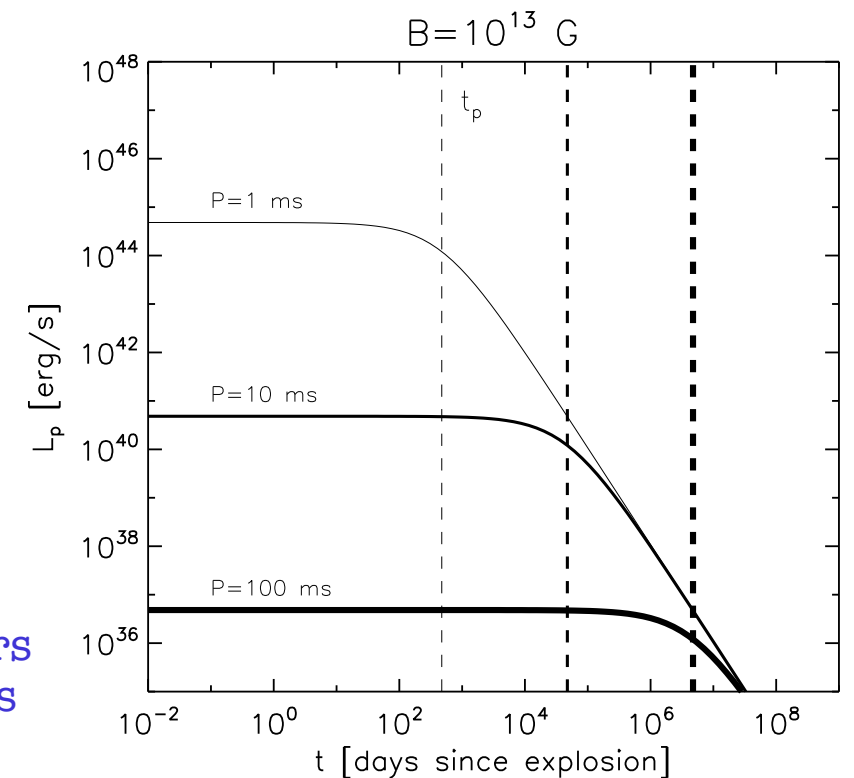
Fang, KK & Olinto (2012, 2013)

Lemoine, KK & Pétri (2015)

outflow energetics

total energy $E_p = \frac{I\Omega_i^2}{2} \sim 1.9 \times 10^{52} \text{ erg } I_{45} P_{i,-3}^2$

neutron star luminosity $L_p(t) = \frac{E_p}{t_p} \frac{1}{(1 + t/t_p)^2}$



$t_p \sim$ a few years
for ms pulsars

conversion of pulsar electromagnetic into kinetic energy

particles accelerated to maximum Lorentz factor:

$$\gamma_M \simeq \frac{L_p}{\dot{N} m c^2} \leftarrow \text{Goldreich-Julian charge density}$$

maximum energy:

$$E_0 \sim 1.5 \times 10^{20} \text{ eV } A_{56} \eta \kappa_4^{-1} P_{i,-3}^{-2} B_{13} R_{\star,6}^3$$

fraction of luminosity into
particle kinetic energy

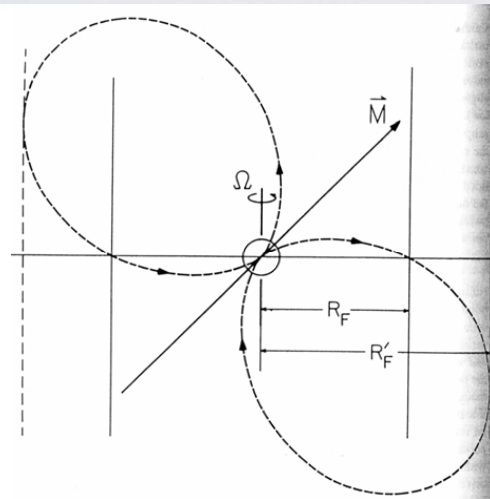
pair
multiplicity

Particle acceleration in pulsars/magnetars

Charge density

Induced electric field

$$\mathbf{E} = -\frac{\mathbf{v}}{c} \times \mathbf{B} = -\frac{1}{c}(\boldsymbol{\Omega} \times \mathbf{r}) \times \mathbf{B}$$



Implies a charge density (Goldreich-Julian 69)

$$\rho = \frac{1}{4\pi} \nabla \cdot \mathbf{E} \approx -\frac{\boldsymbol{\Omega} \cdot \mathbf{B}}{2\pi c} \equiv \rho_{GJ}$$

e.g.

Blasi et al. (2000)

Arons et al. (2003)

Bednarek & Bartosik (2006)

Fang, KK & Olinto (2012, 2013)

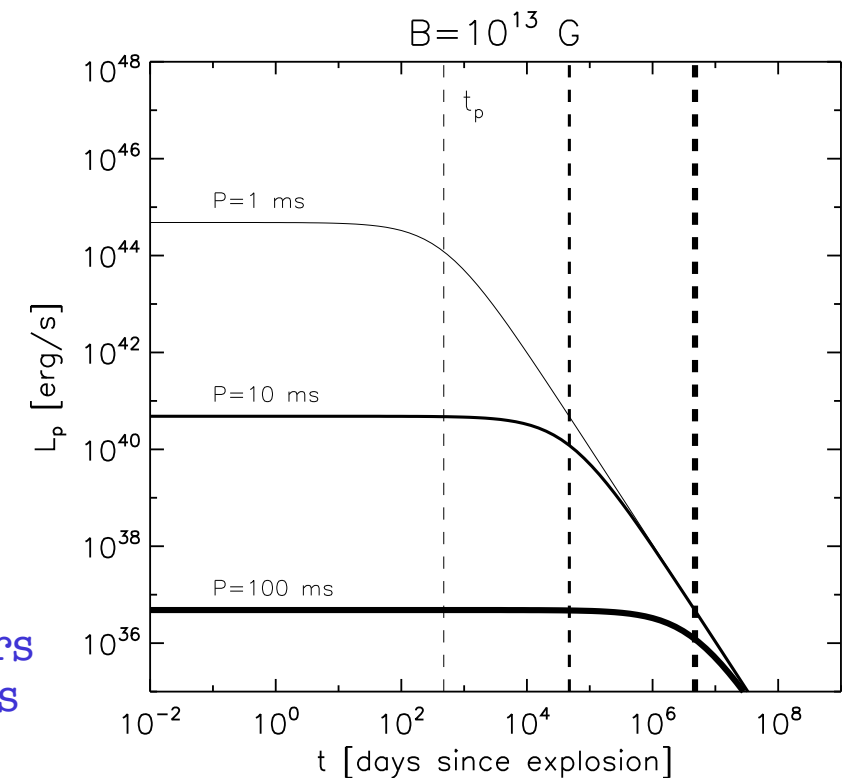
Lemoine, KK & Pétri (2015)

Pulsars born with ms periods and magnetars are good candidates of UHECR sources

outflow energetics

total energy $E_p = \frac{I\Omega_i^2}{2} \sim 1.9 \times 10^{52} \text{ erg } I_{45} P_{i,-3}^2$

neutron star luminosity $L_p(t) = \frac{E_p}{t_p} \frac{1}{(1 + t/t_p)^2}$



$t_p \sim$ a few years for ms pulsars

conversion of pulsar electromagnetic into kinetic energy

particles accelerated to maximum Lorentz factor:

$$\gamma_M \simeq \frac{L_p}{\dot{N} m c^2} \leftarrow \text{Goldreich-Julian charge density}$$

maximum energy:

$$E_0 \sim 1.5 \times 10^{20} \text{ eV } A_{56} \eta \kappa_4^{-1} P_{i,-3}^{-2} B_{13} R_{\star,6}^3$$

fraction of luminosity into particle kinetic energy

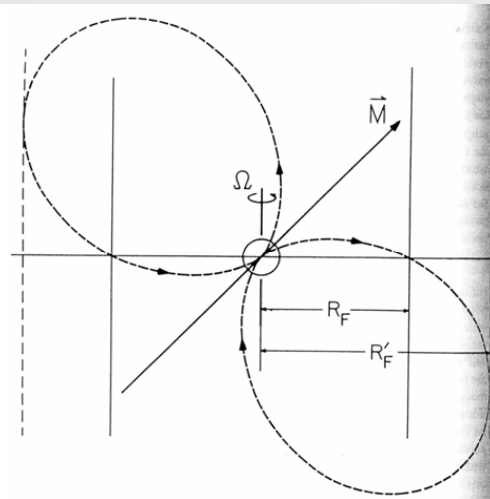
pair multiplicity

Particle acceleration in pulsars/magnetars

Charge density

Induced electric field

$$\mathbf{E} = -\frac{\mathbf{v}}{c} \times \mathbf{B} = -\frac{1}{c}(\boldsymbol{\Omega} \times \mathbf{r}) \times \mathbf{B}$$



Implies a charge density (Goldreich-Julian 69)

$$\rho = \frac{1}{4\pi} \nabla \cdot \mathbf{E} \approx -\frac{\boldsymbol{\Omega} \cdot \mathbf{B}}{2\pi c} \equiv \rho_{GJ}$$

e.g.

Blasi et al. (2000)

Arons et al. (2003)

Bednarek & Bartosik (2006)

Fang, KK & Olinto (2012, 2013)

Lemoine, KK & Pétri (2015)

composition

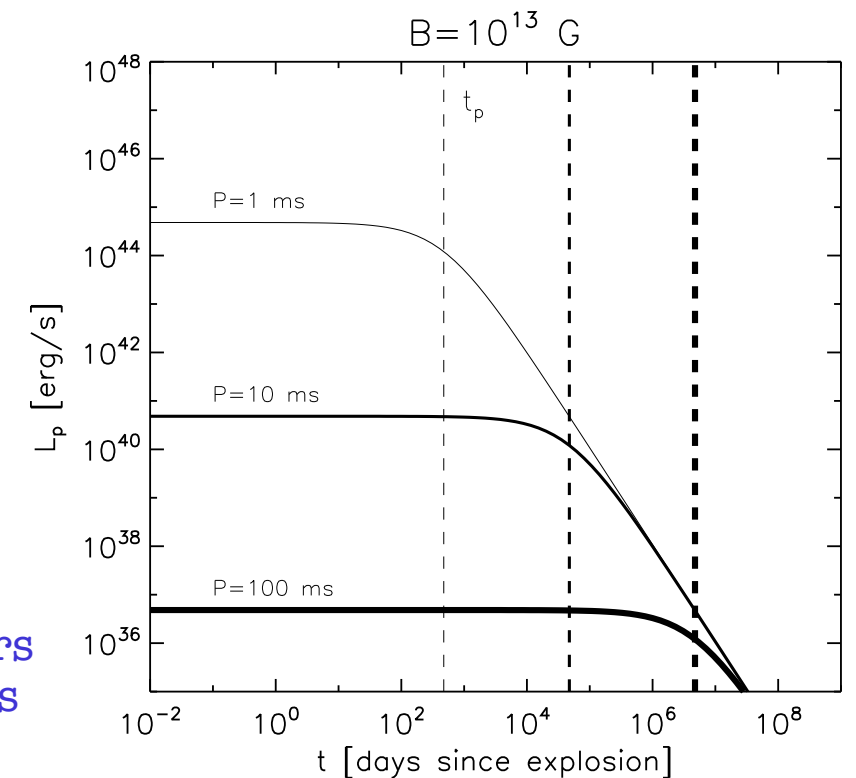
neutron stars have metal-rich surfaces:
ideal site for heavy nuclei production

Pulsars born with ms periods
and magnetars are good
candidates of UHECR sources

outflow energetics

total energy $E_p = \frac{I\Omega_i^2}{2} \sim 1.9 \times 10^{52} \text{ erg } I_{45} P_{i,-3}^2$

neutron star luminosity $L_p(t) = \frac{E_p}{t_p} \frac{1}{(1 + t/t_p)^2}$



$t_p \sim$ a few years
for ms pulsars

conversion of pulsar electromagnetic into kinetic energy

particles accelerated to maximum Lorentz factor:

$$\gamma_M \simeq \frac{L_p}{\dot{N} m c^2} \leftarrow \text{Goldreich-Julian charge density}$$

maximum energy:

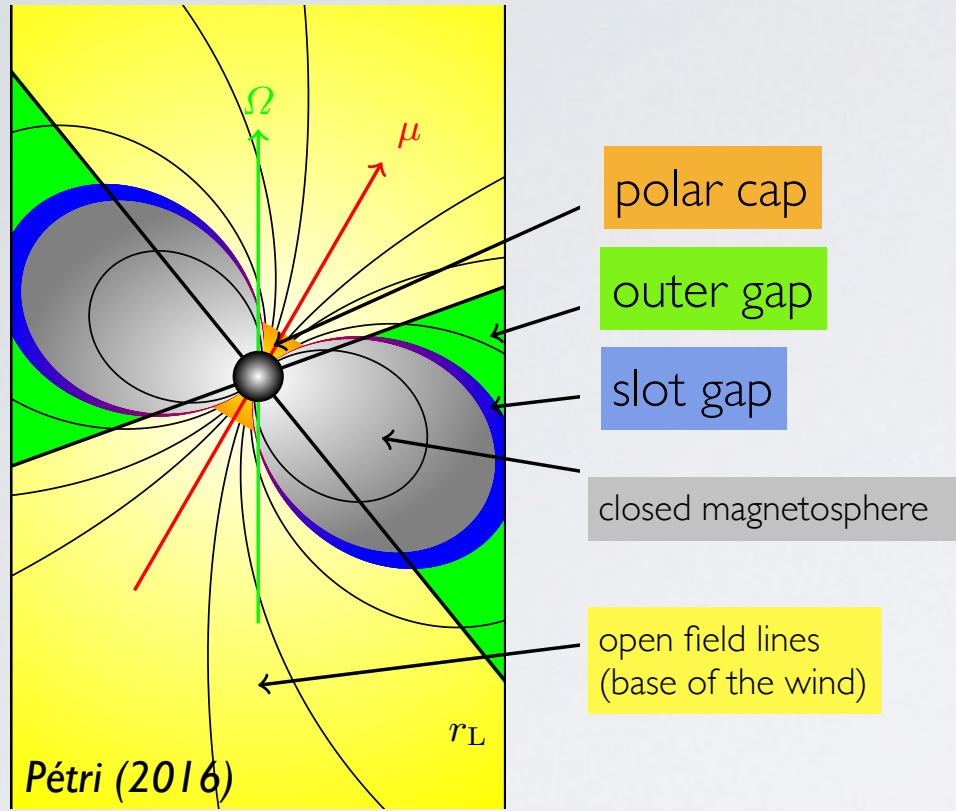
$$E_0 \sim 1.5 \times 10^{20} \text{ eV } A_{56} \eta \kappa_4^{-1} P_{i,-3}^{-2} B_{13} R_{\star,6}^3$$

fraction of luminosity into
particle kinetic energy

pair
multiplicity

Cosmic ray acceleration in pulsars

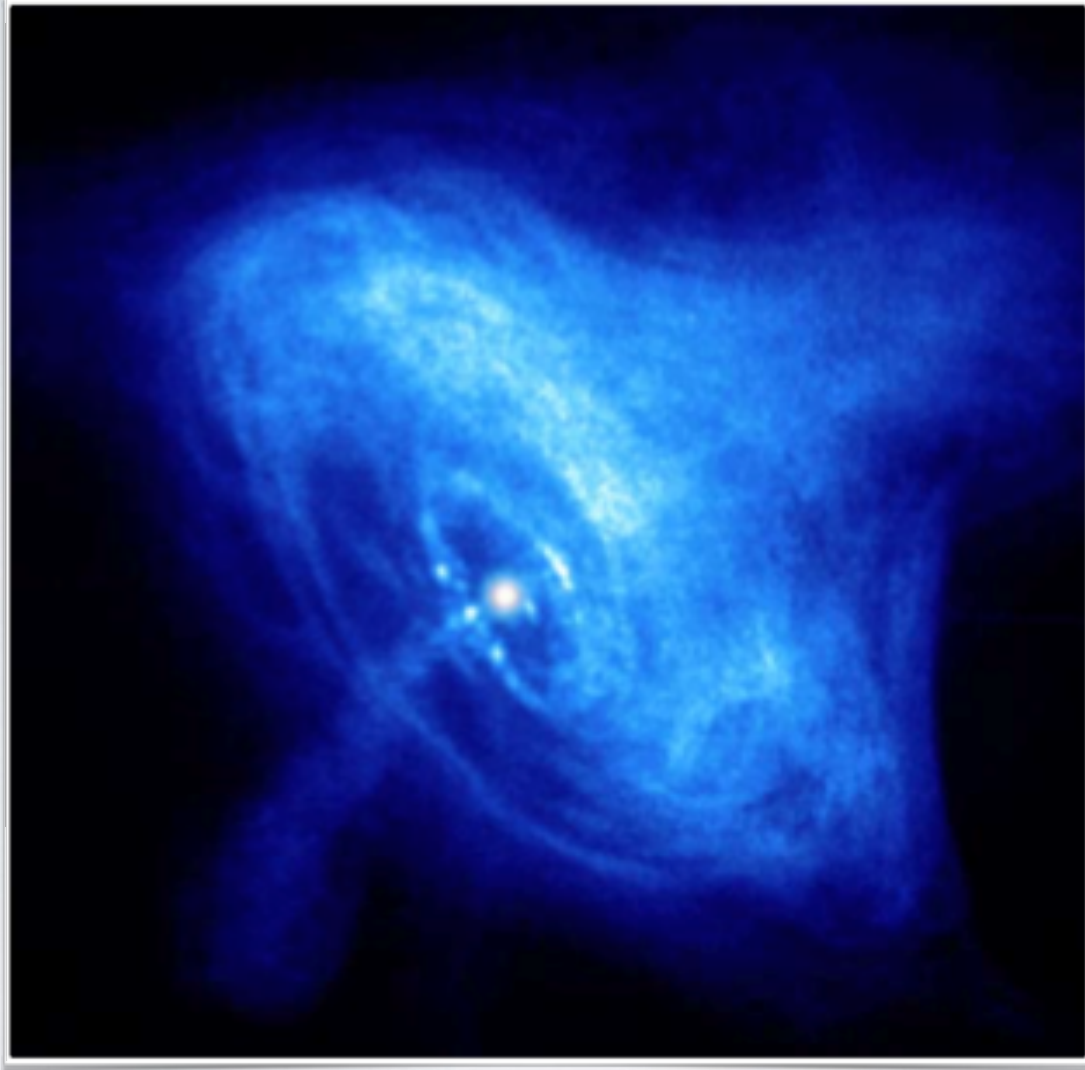
► Acceleration region?



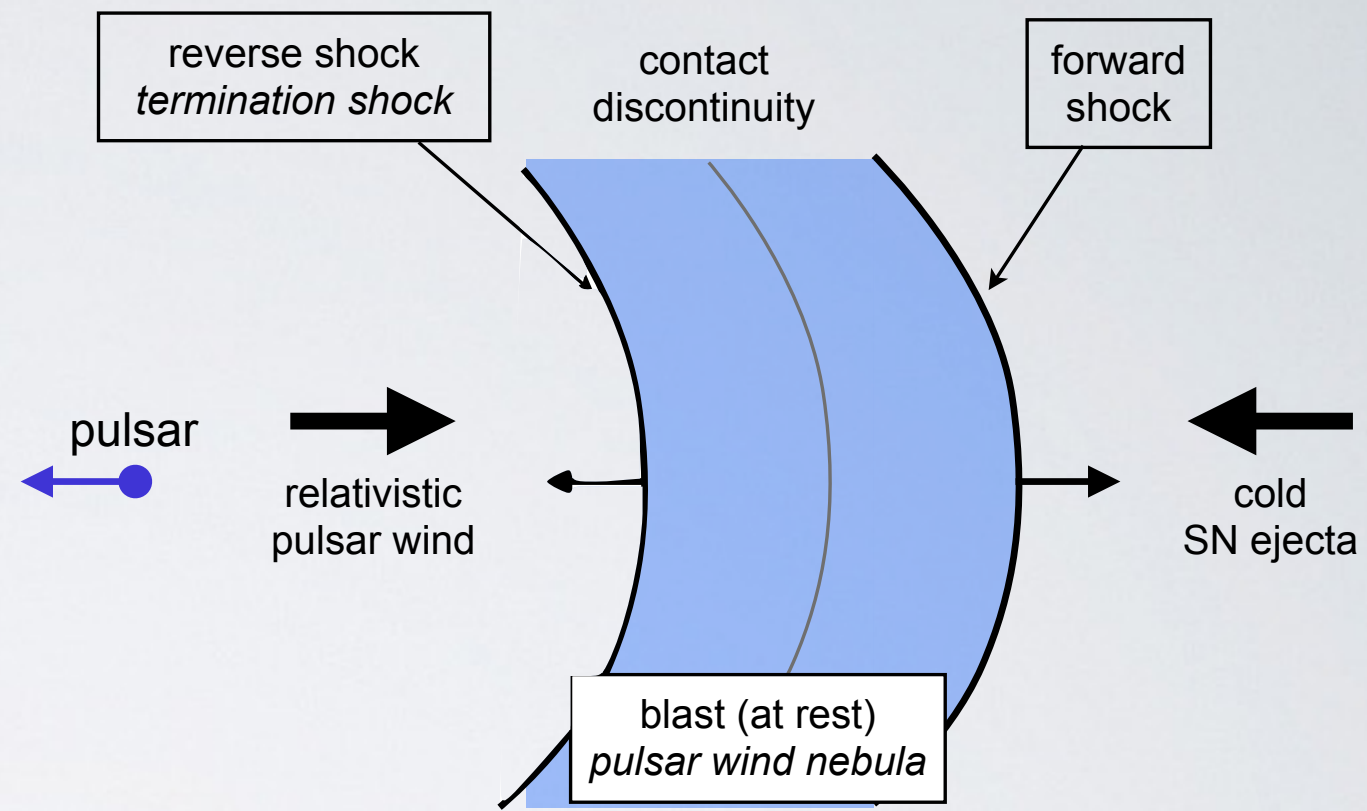
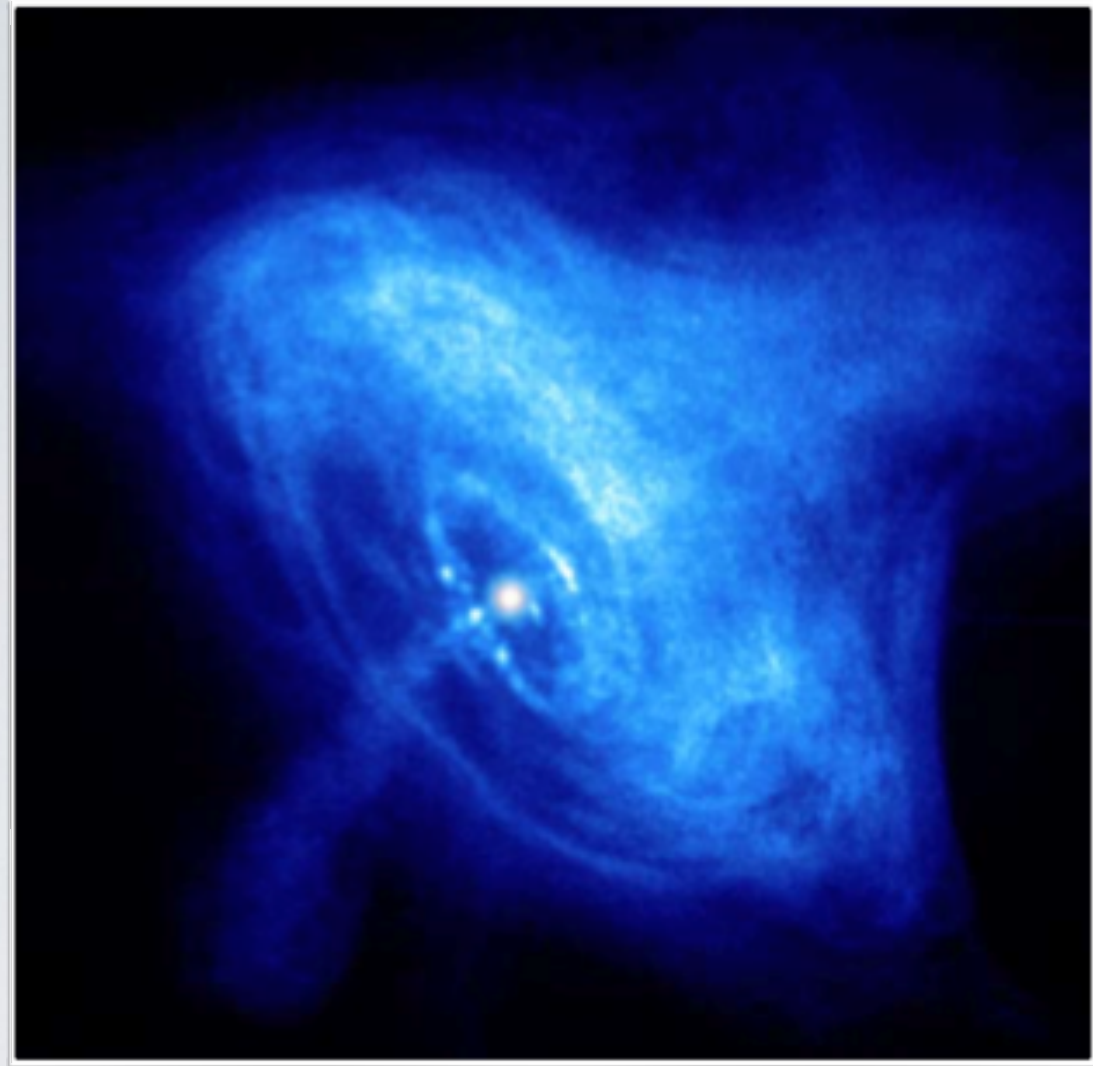
► Gaps close to star

reviews: *Harding (2007), Hirotani (2008)*

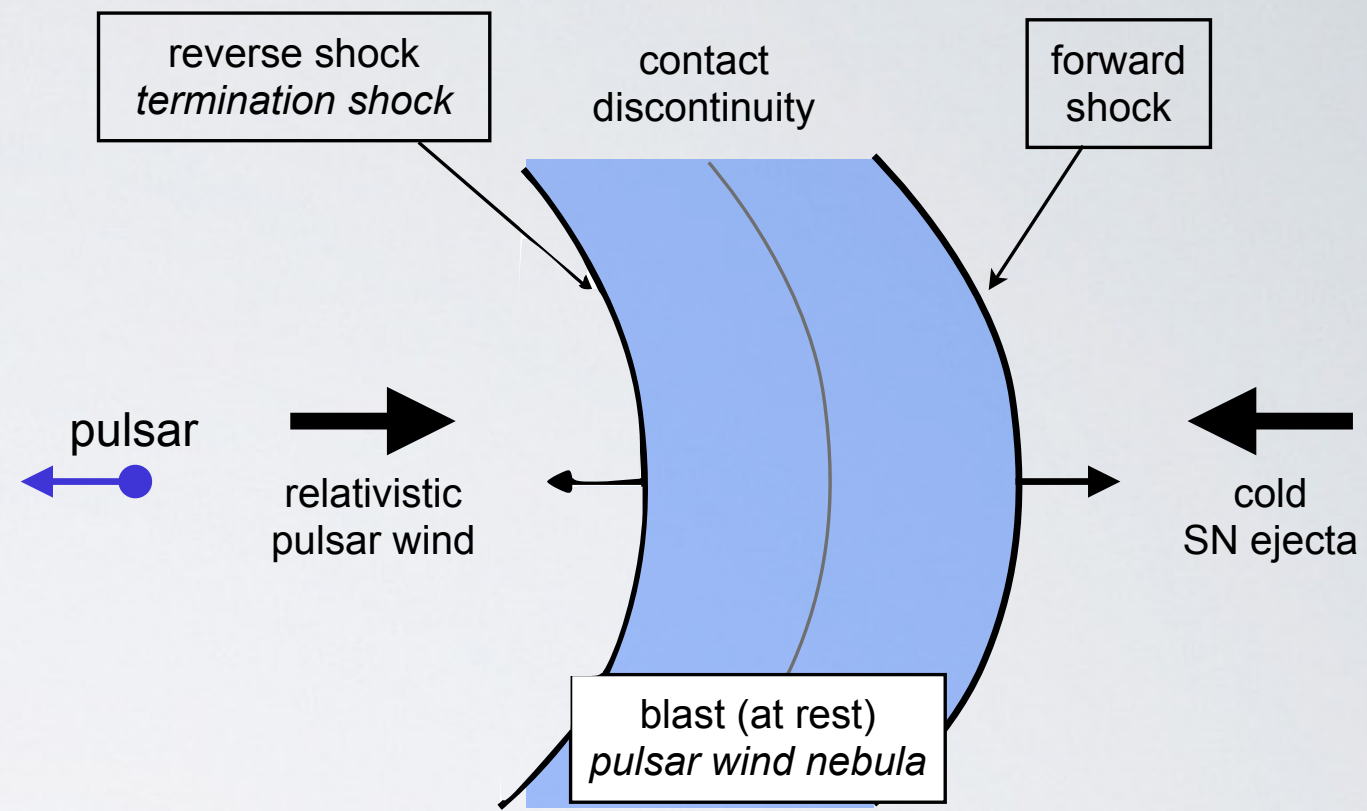
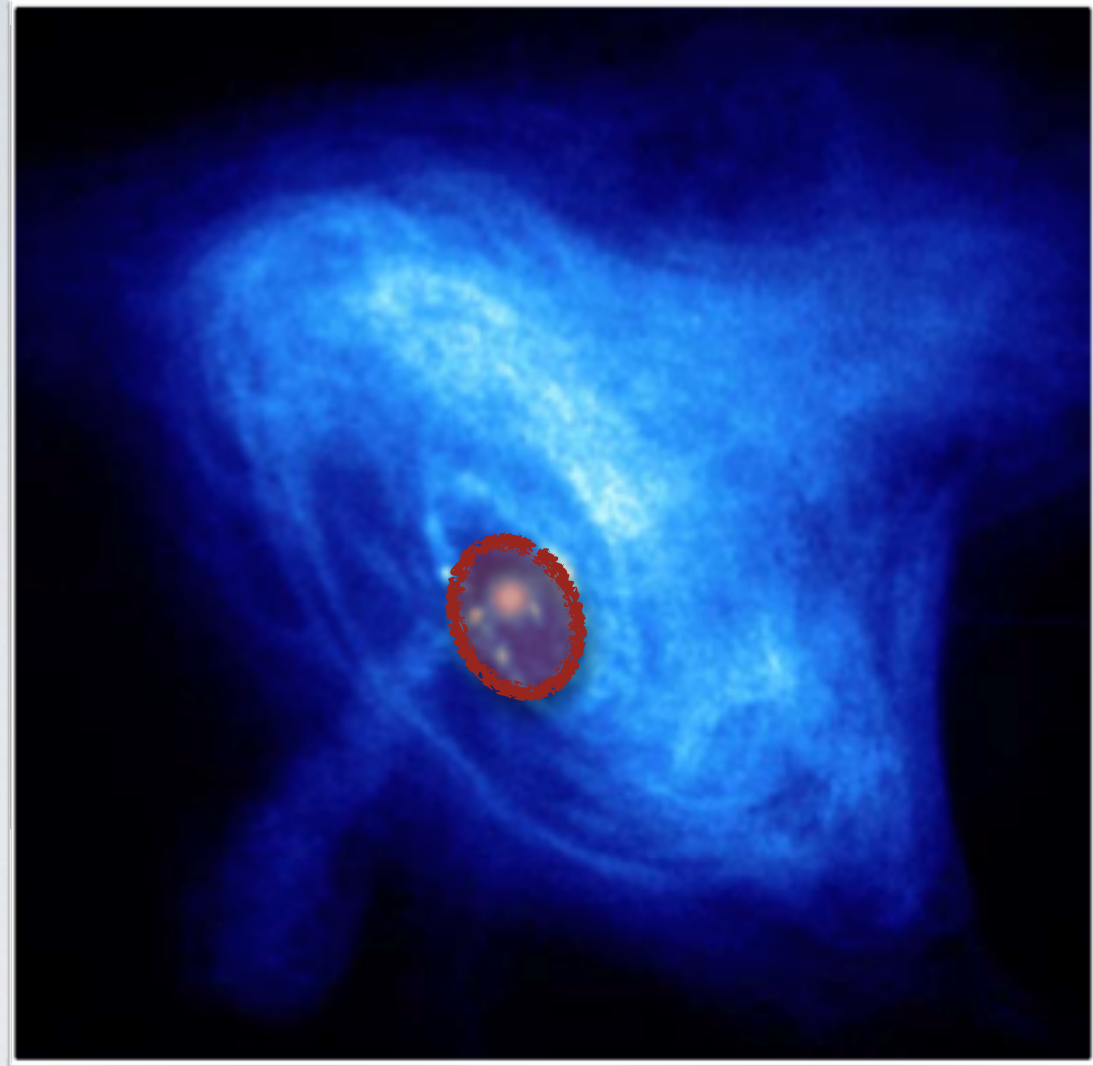
► Acceleration region?



► Acceleration region?

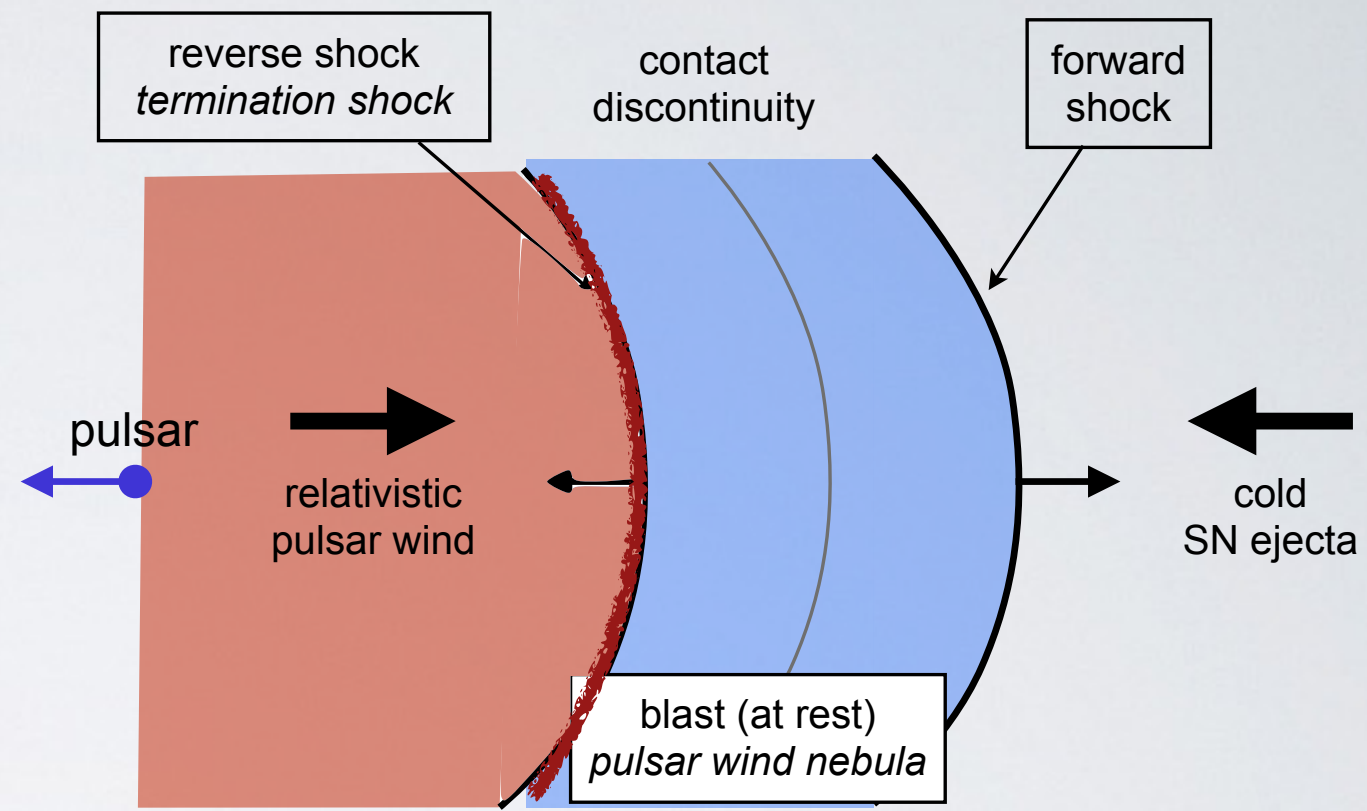
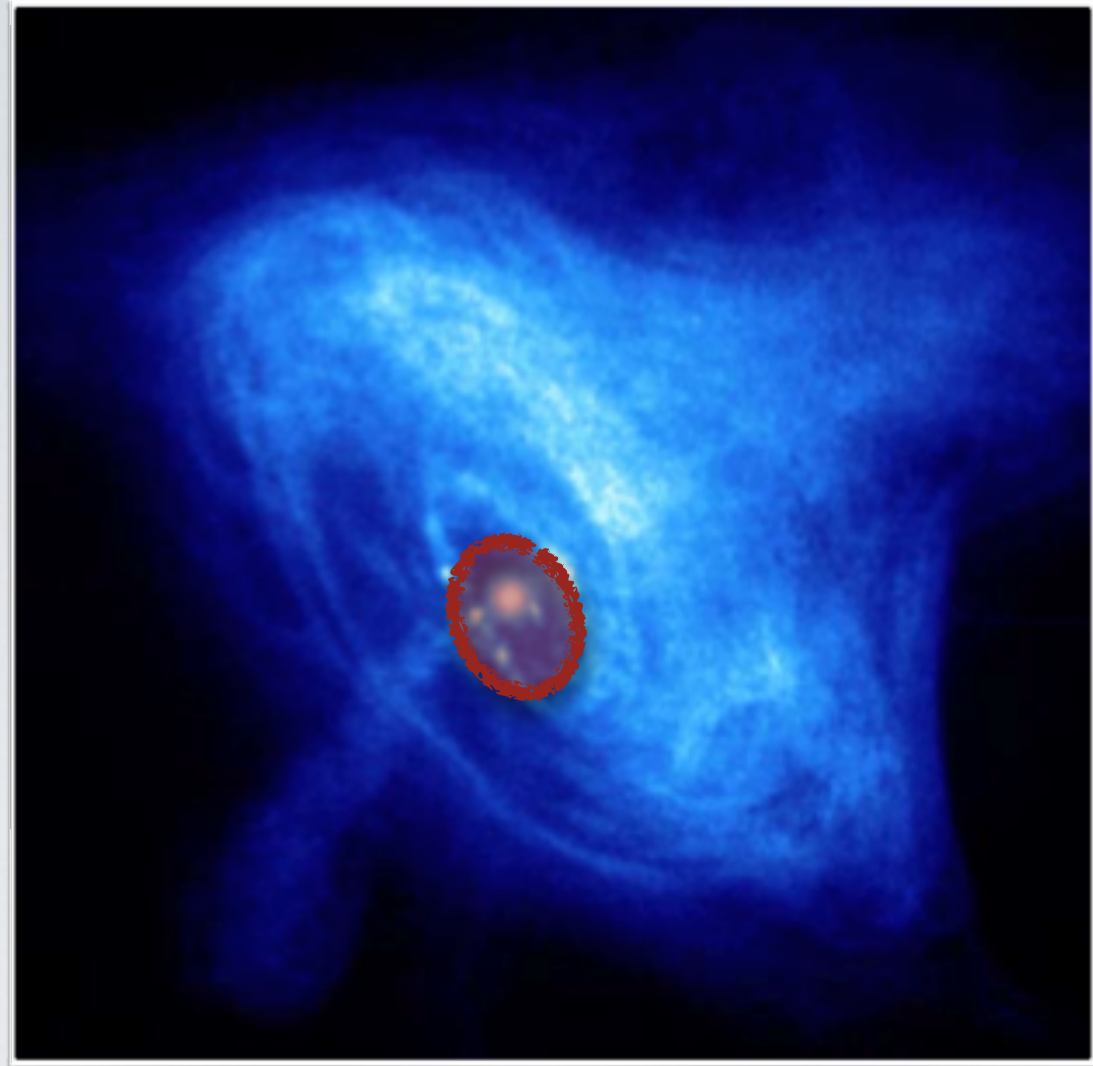


► Acceleration region?



Cosmic ray acceleration in pulsars

► Acceleration region?

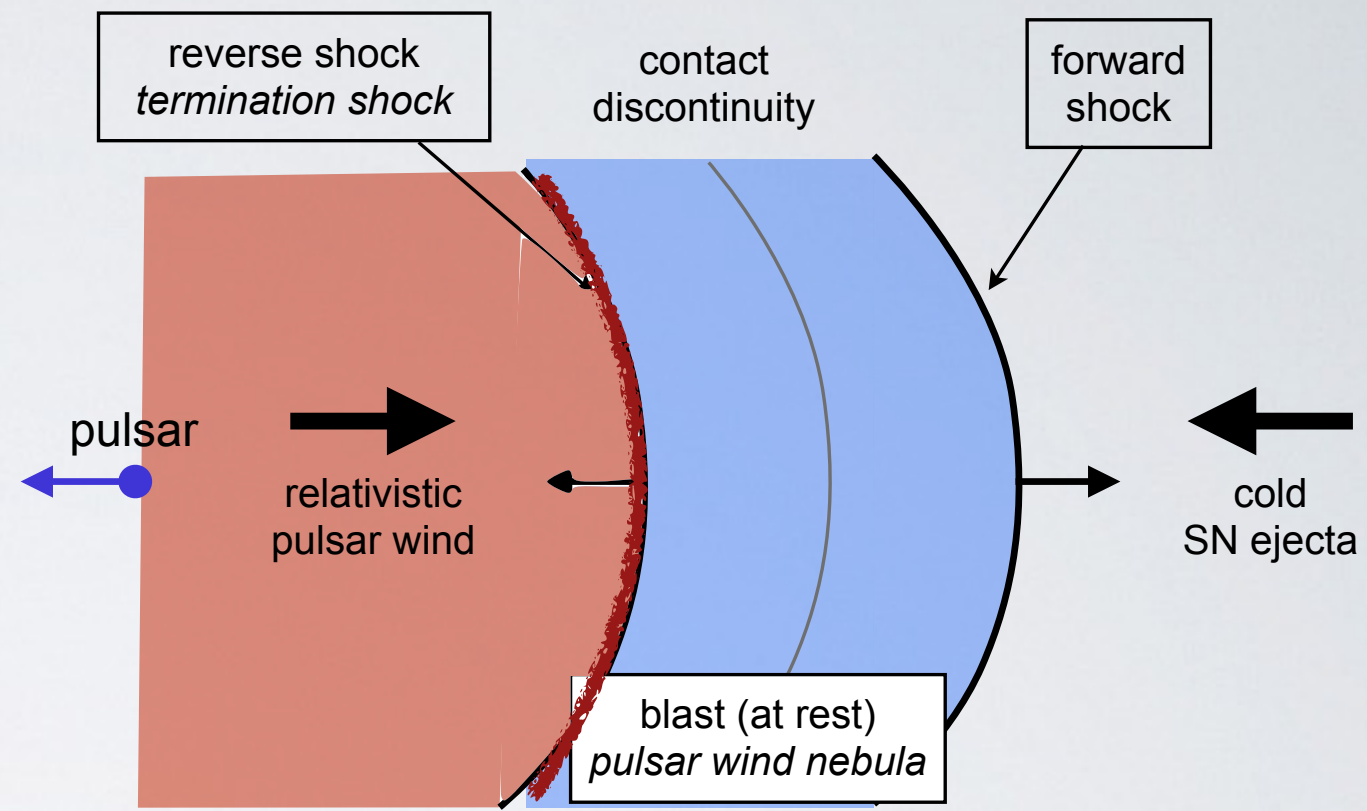
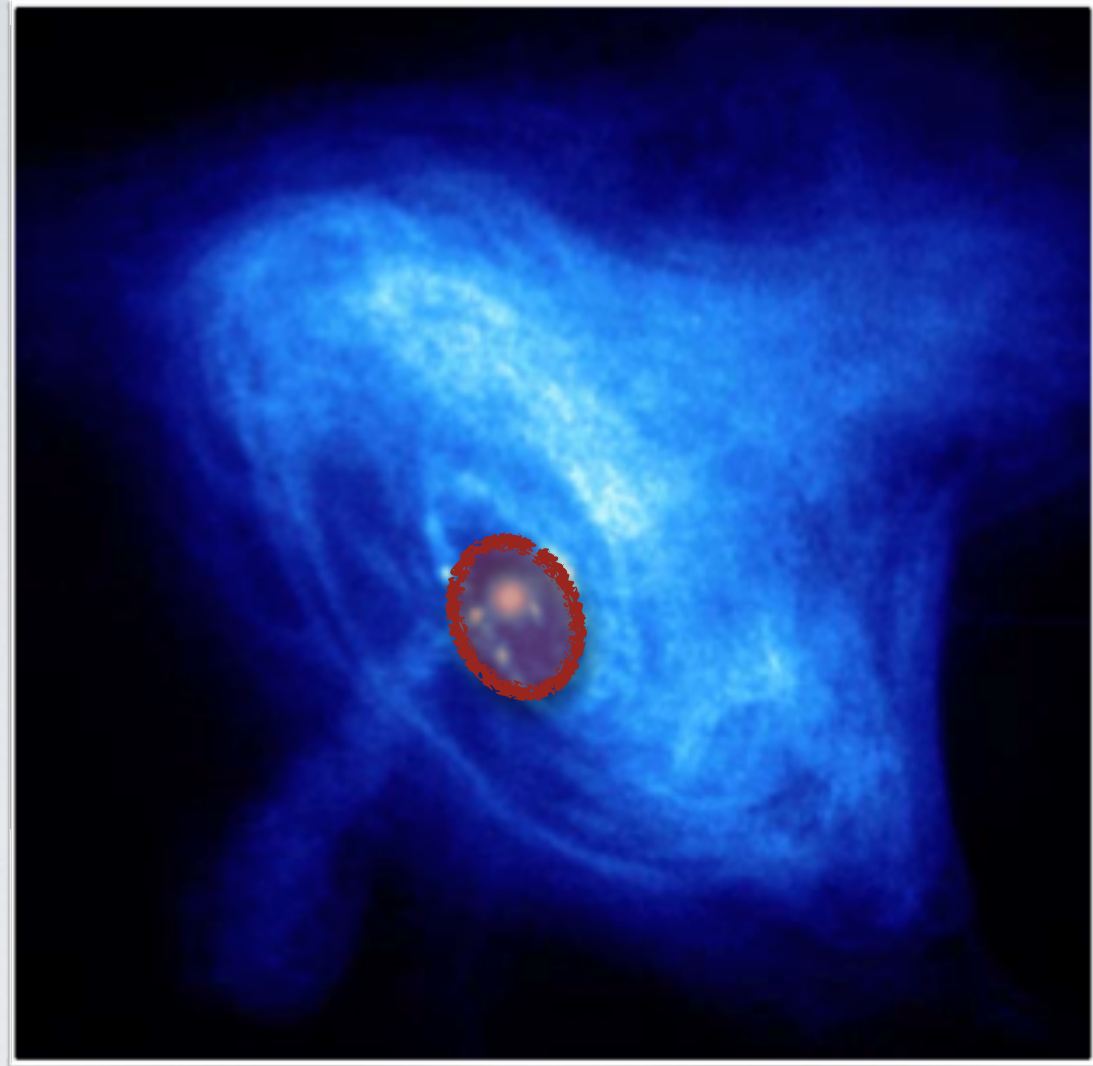


► Wind region

cold
Poynting flux
dominated?

Cosmic ray acceleration in pulsars

► Acceleration region?



► Wind region

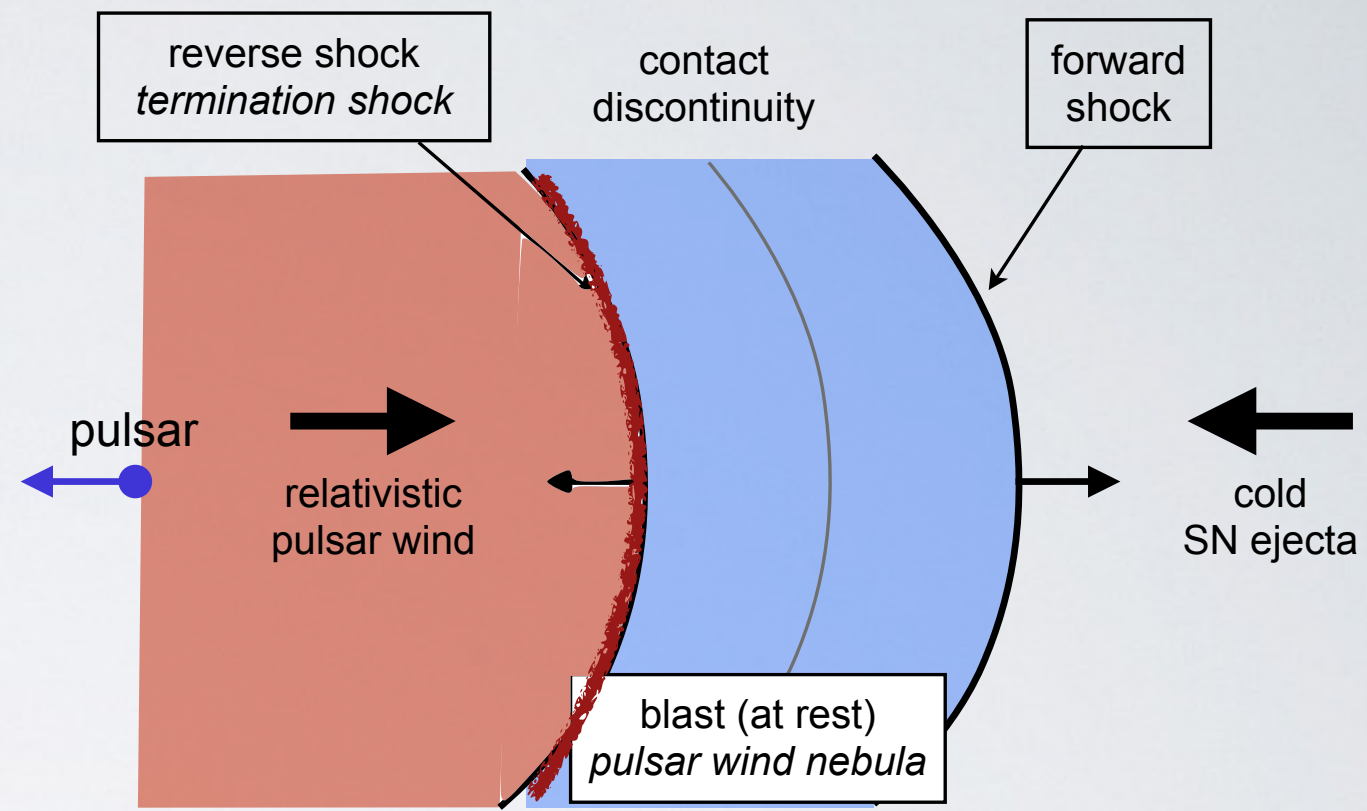
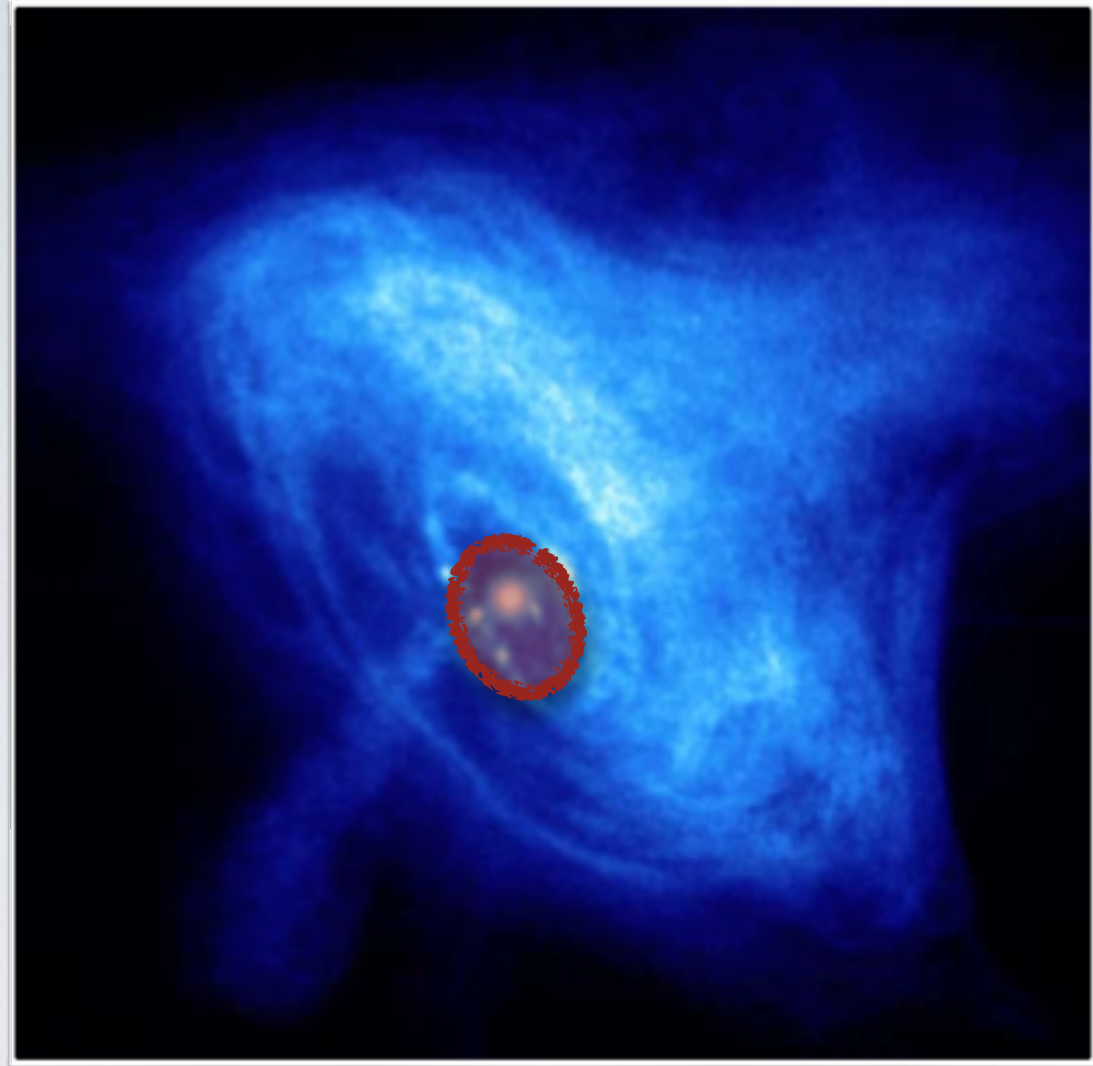
cold
Poynting flux
dominated?

► Nebula

radiative
kinetic energy

Cosmic ray acceleration in pulsars

► Acceleration region?



► Wind region

► Nebula

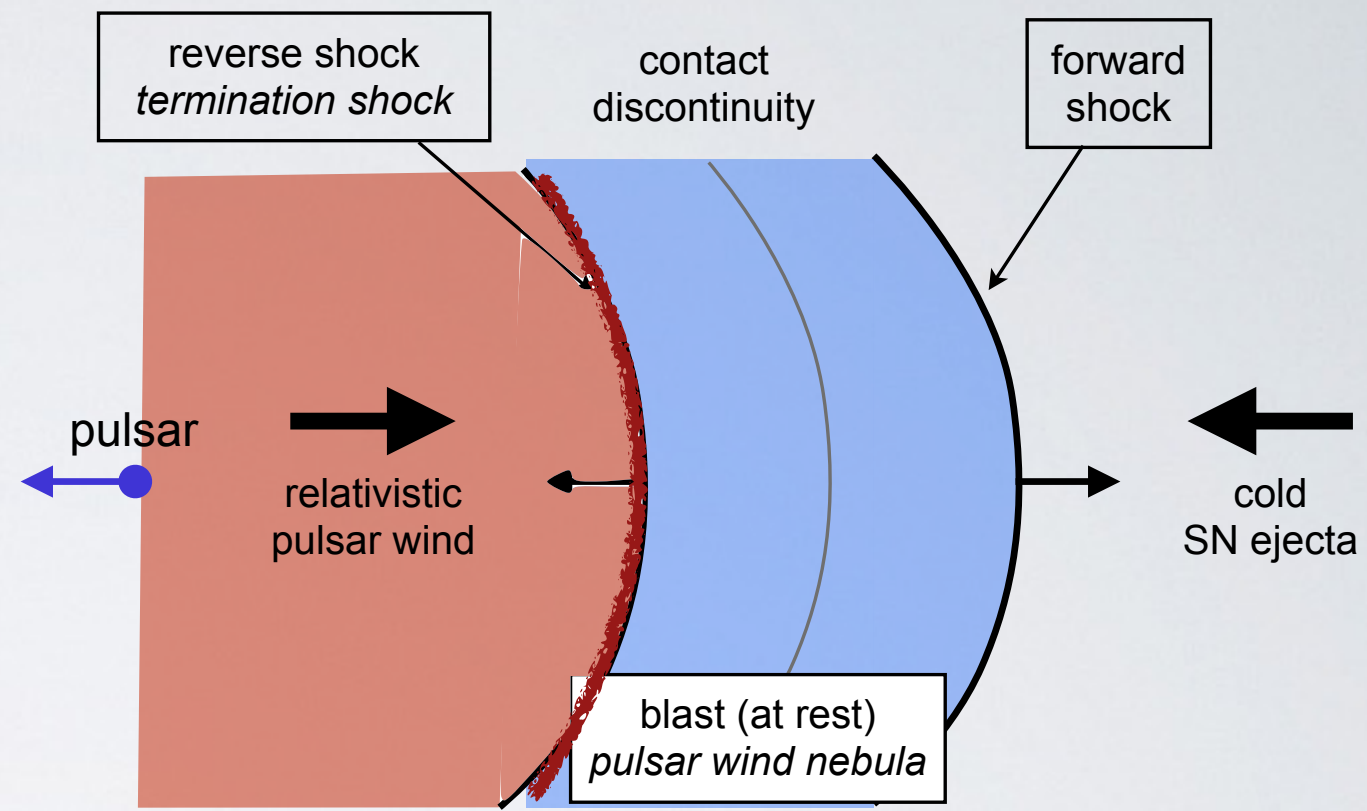
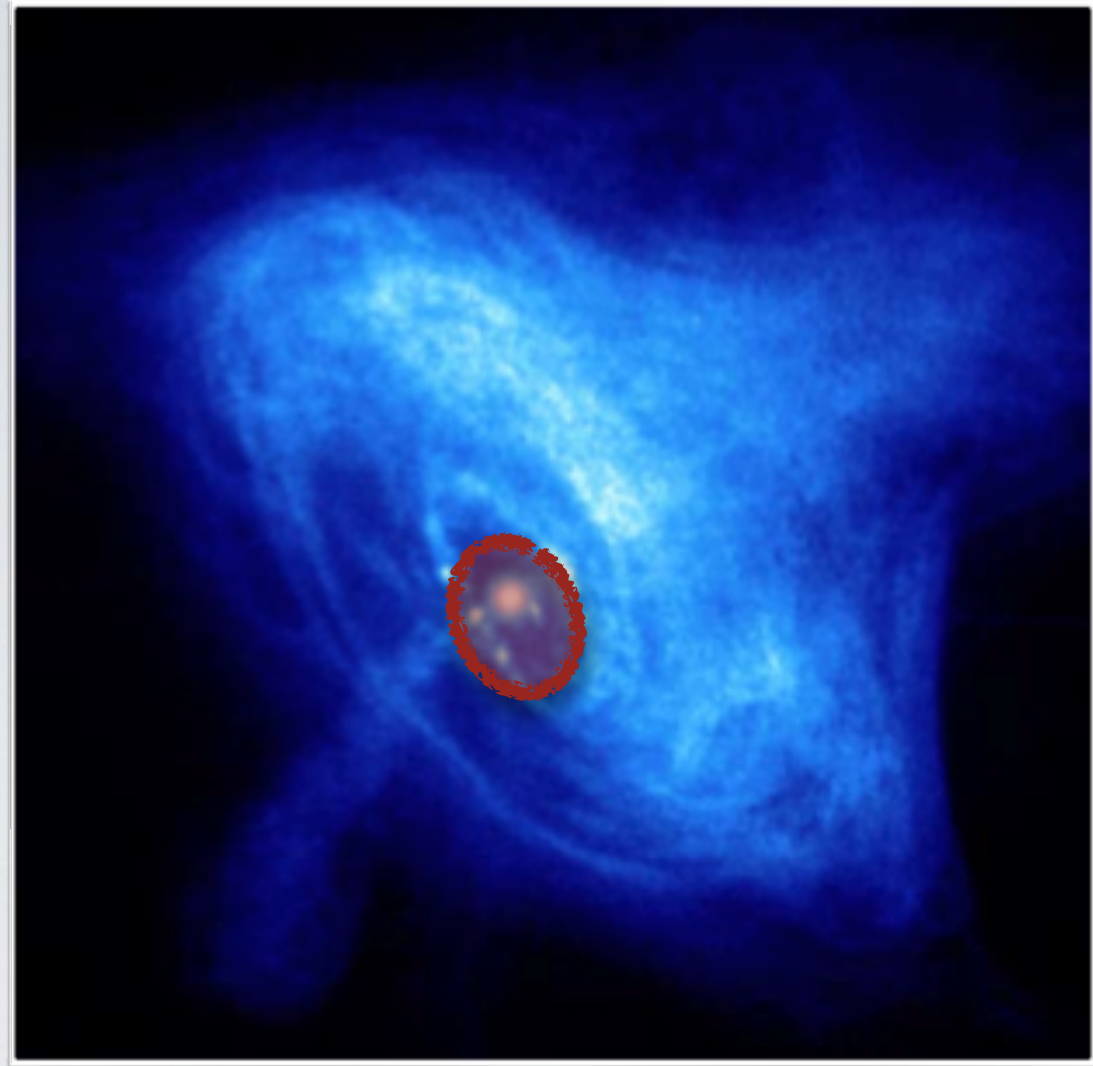
cold
Poynting flux
dominated?

radiative
kinetic energy

- dissipation of e-m to kinetic energy?
- related to "sigma-problem"

e.g., Kirk et al. 2009

► Acceleration region?



► Wind region

► Nebula

cold
Poynting flux
dominated?

radiative
kinetic energy

- dissipation of e-m to kinetic energy?
- related to "sigma-problem"

e.g., Kirk et al. 2009

► Acceleration mechanism?

- « linear » $E \propto r$ e.g., Chen et al. 92, Arons 03
- Fermi @ TS e.g., Lemoine, KK, Pétri 15
- reconnection wind region and/or close to TS in striped wind or in nebula? e.g., Sironi & Spitkovsky 12, Lemoine, KK, Pétri 15

Interaction backgrounds for neutrino production

nebula non-thermal γ

Amato et al. (2003)
Lemoine, KK, Pétri (2015)

SN thermal γ

Amato et al. (2003)
Fang, KK, Murase & Olinto (2016)

SN ejecta matter

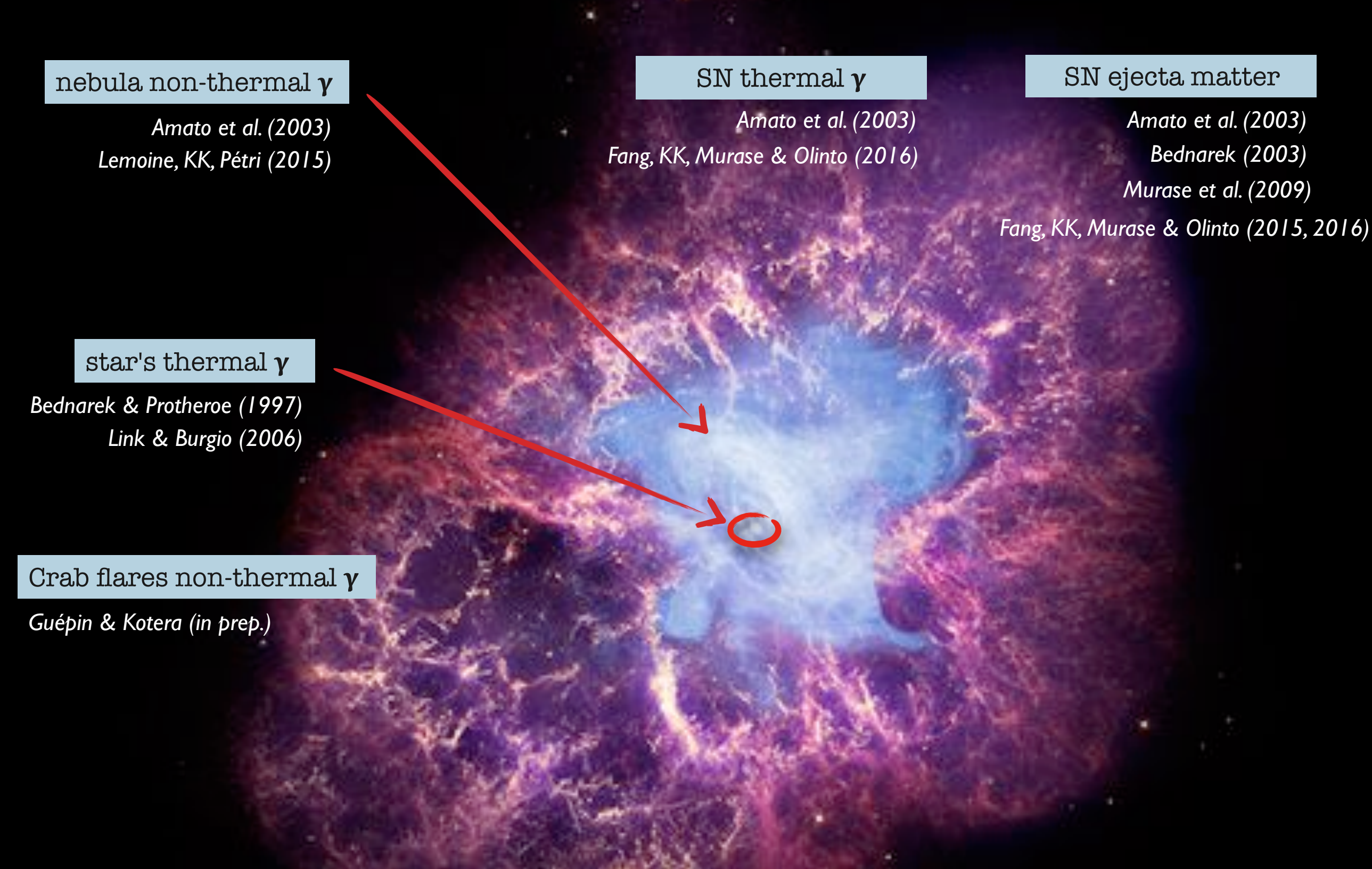
Amato et al. (2003)
Bednarek (2003)
Murase et al. (2009)
Fang, KK, Murase & Olinto (2015, 2016)

star's thermal γ

Bednarek & Protheroe (1997)
Link & Burgio (2006)

Crab flares non-thermal γ

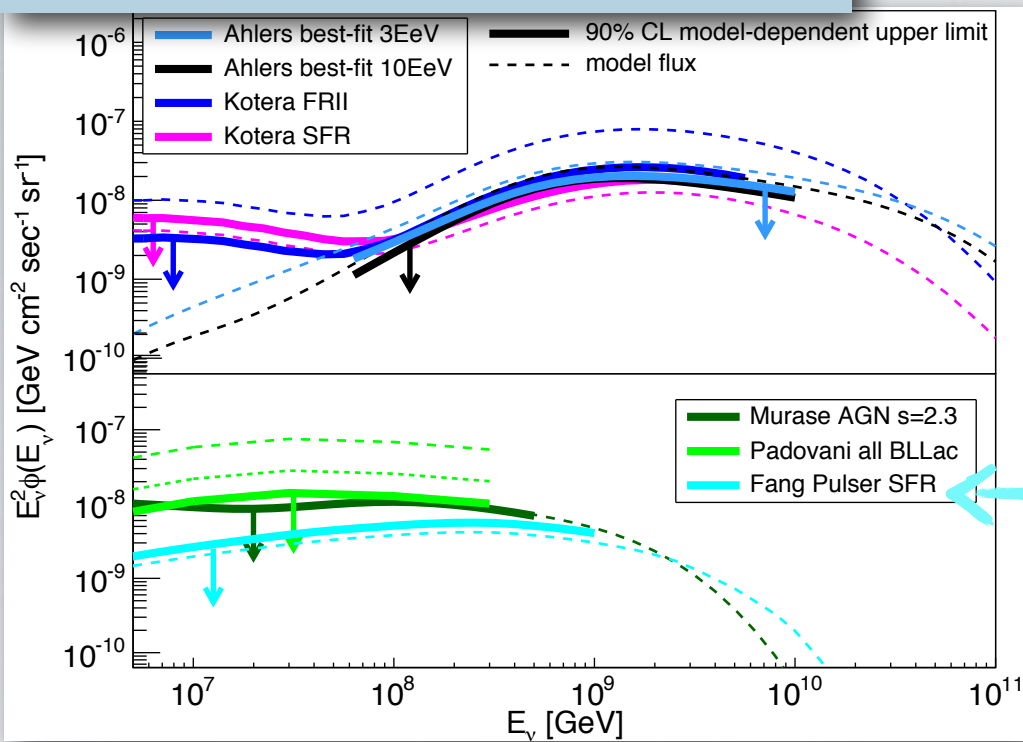
Guépin & Kotera (in prep.)



► Most promising for UHECRs: interactions in SN

IceCube constraints on neutron stars as sources of UHECRs

model dependent 90% C.L. limits



► Population of newborn pulsars as sources of UHECRs following star formation rate excluded at 90% C.L.

population of pulsars with realistic (P,B) distribution

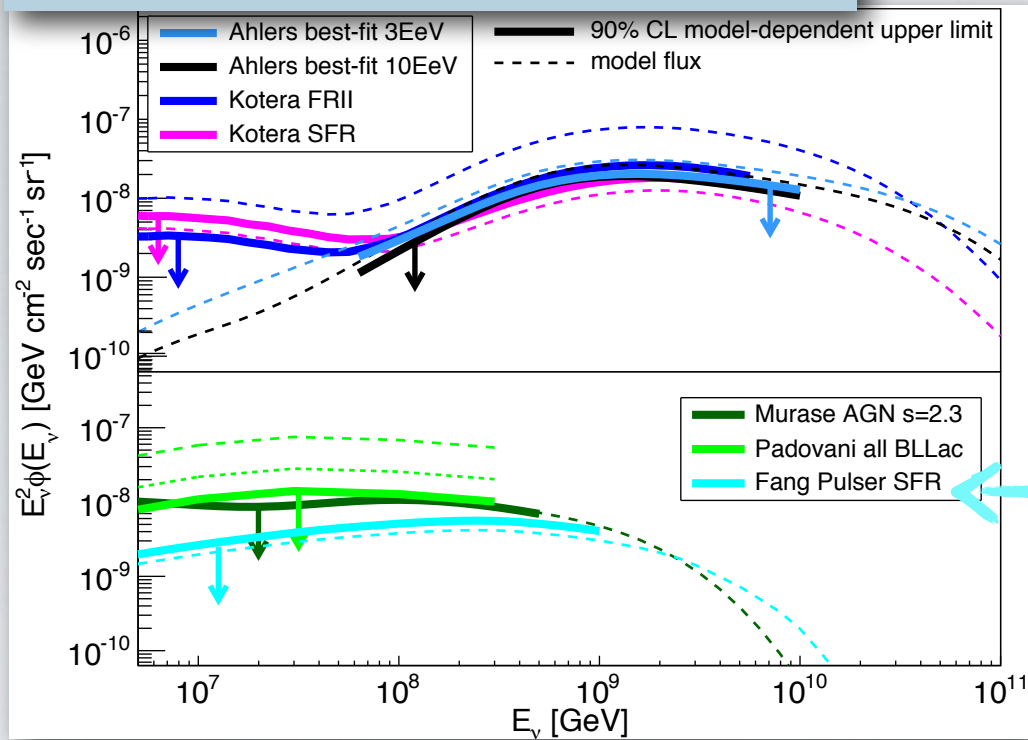
A. Ishihara's talk

Fang, KK, Murase & Olinto 2013

Aartsen et al. 2016

IceCube constraints on neutron stars as sources of UHECRs

model dependent 90% C.L. limits



Aartsen et al. 2016

Population of newborn pulsars as sources of UHECRs following star formation rate excluded at 90% C.L.

population of pulsars with realistic (P,B) distribution

A. Ishihara's talk

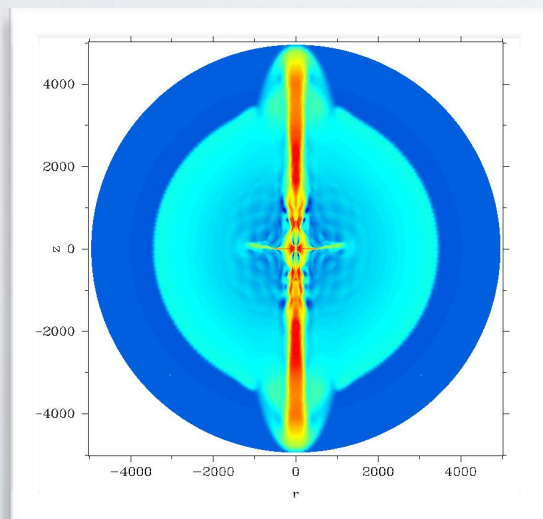
Fang, KK, Murase & Olinto 2013

neutrino fluxes @ break energy, if normalized to UHECR spectrum

Fang, KK, Murase & Olinto 2016

population of neutron stars with same characteristics (P,B)

magnetar jet puncturing SN ejecta

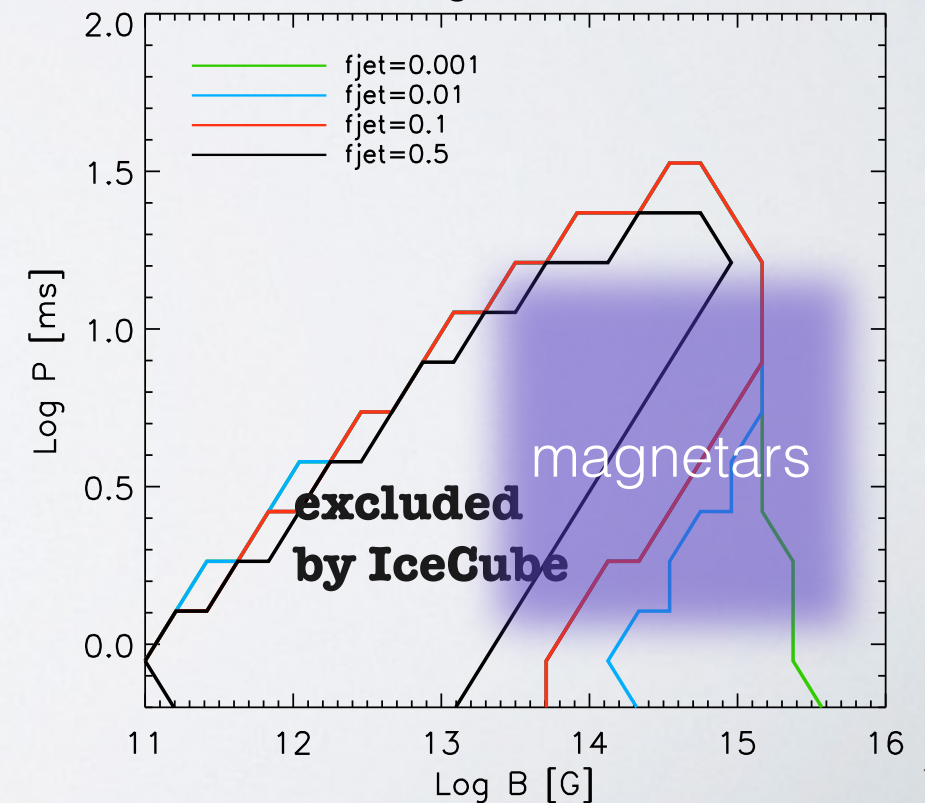


Komissarov & Barkov (2007)

f_{jet} = "jet fraction"

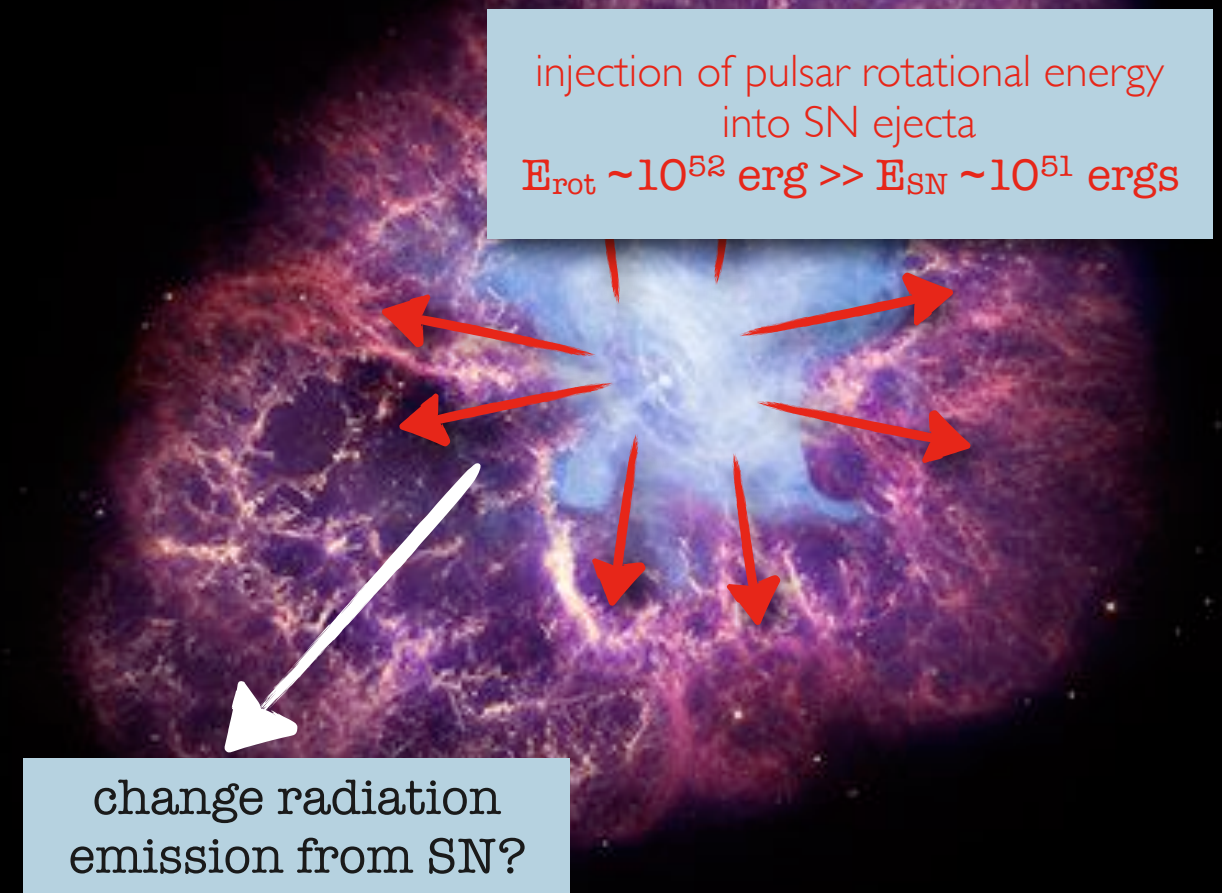
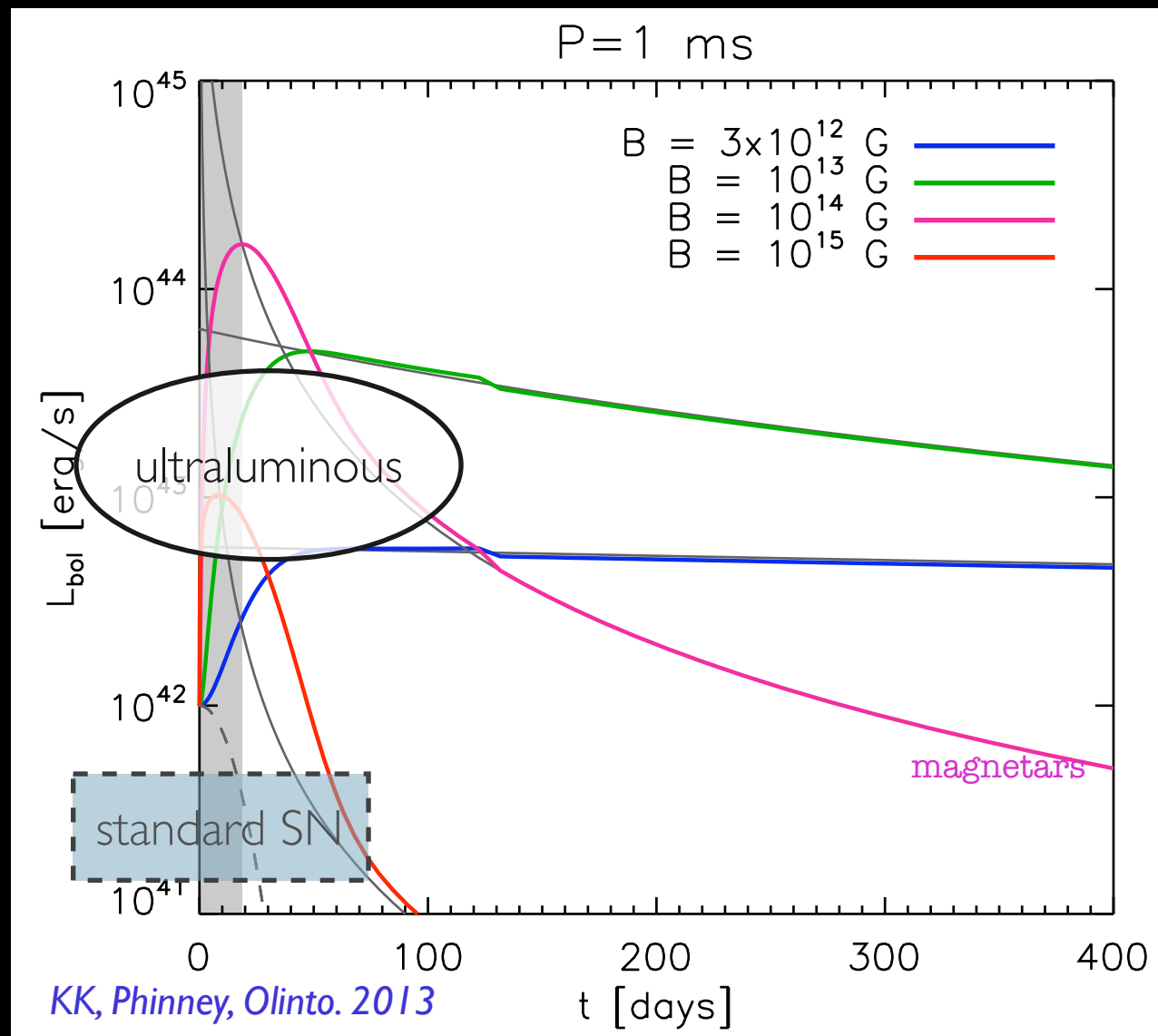
fraction of accelerated particles that can escape without crossing a dense environment

magnetars not excluded if escape fraction > 10%
UHECR production and escape possible



Superluminous supernovae due to central pulsar/magnetar

▶ superluminous supernovae lasting over a few days/months/years



Superluminous supernovae due to central pulsar/magnetar

▶ superluminous supernovae lasting over a few days/months/years

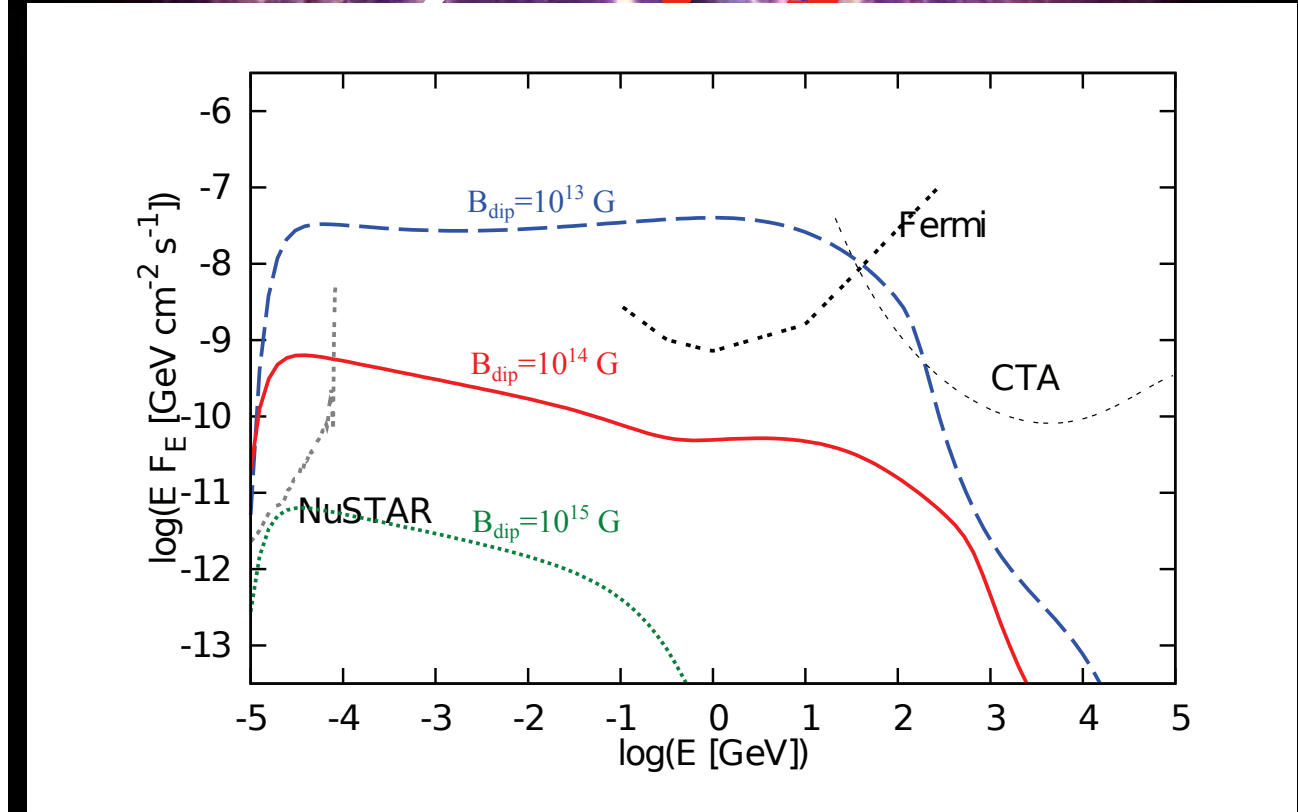
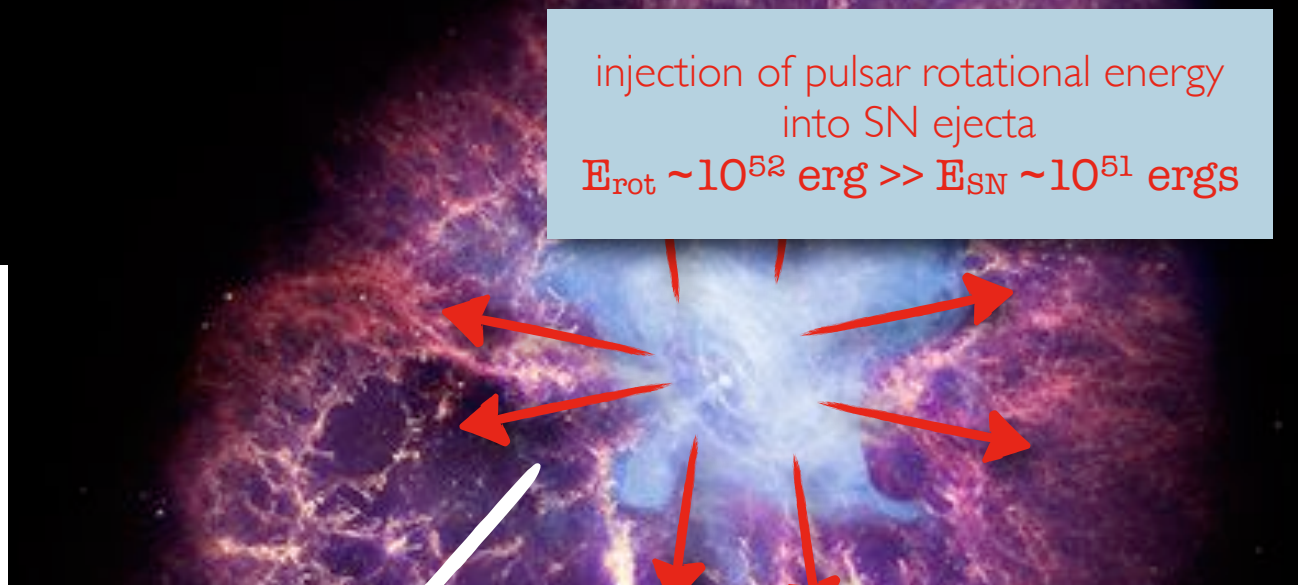
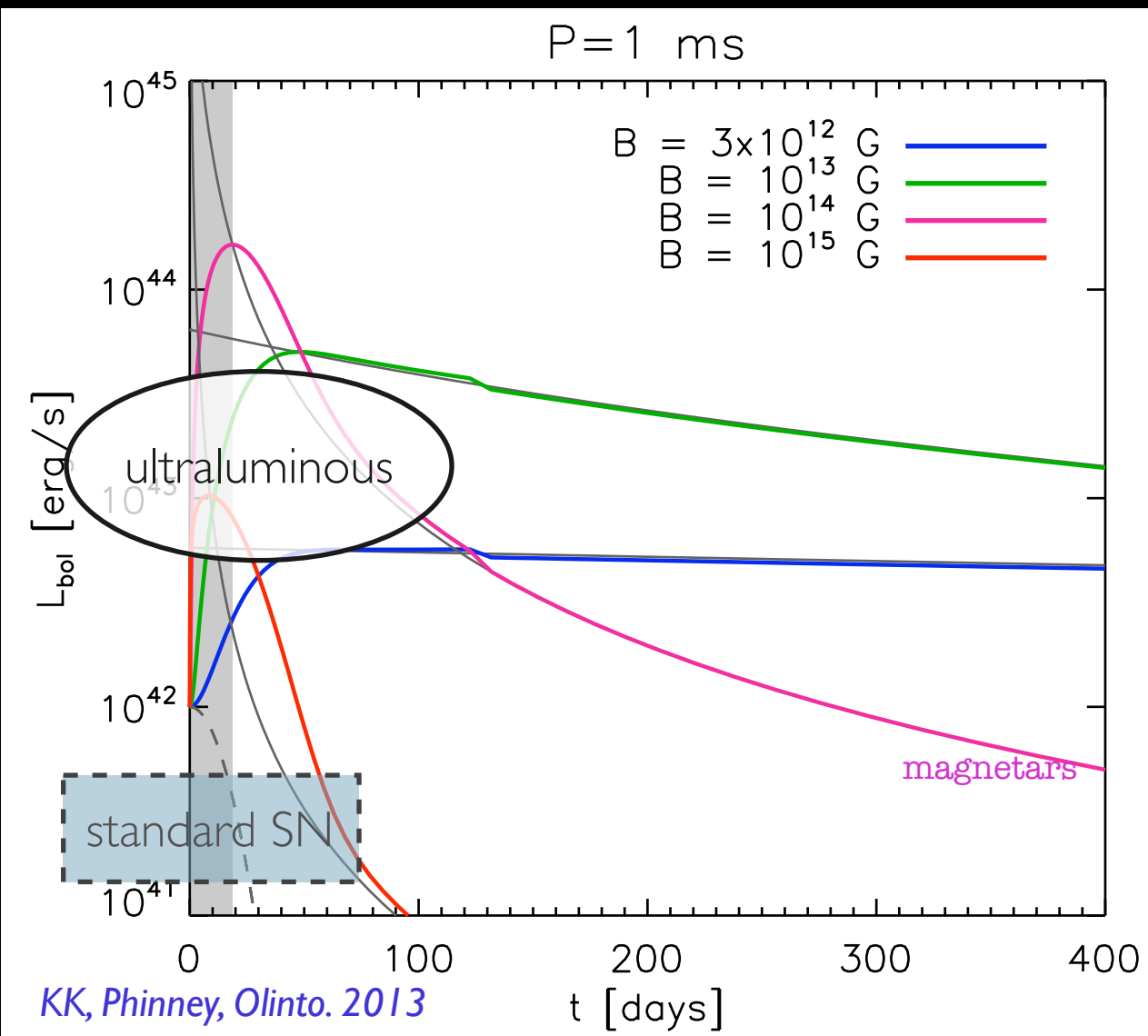


FIG. 7.— High-energy photon spectra of the early PWN embedded in the SN ejecta for $P_i = 2$ ms at $t = 10^{7.5}$ s ≈ 316 d. Different magnetic field strengths are considered. Detections with CTA are possible for $B_{\text{dip}} = 10^{13}$ G.

Murase et al. 2015

Superluminous supernovae due to central pulsar/magnetar

▶ superluminous supernovae lasting over a few days/months/years

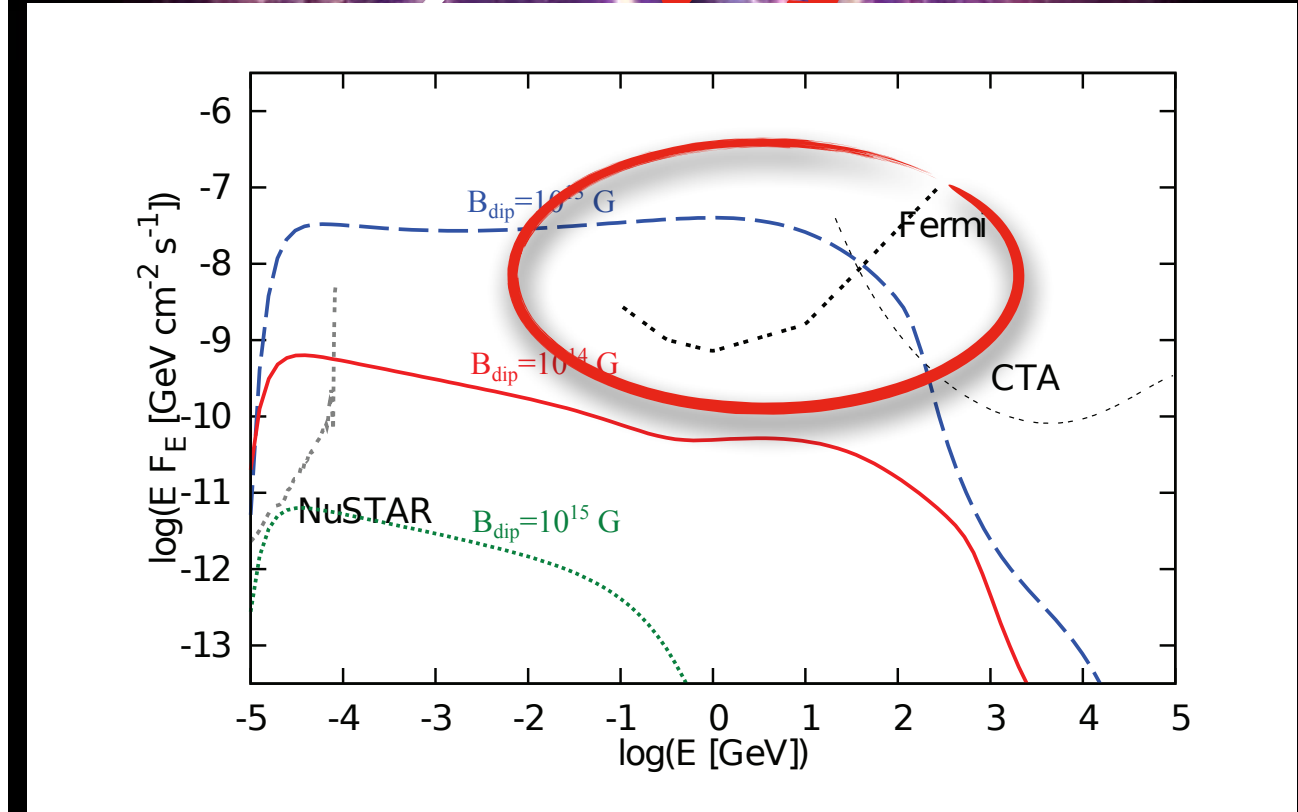
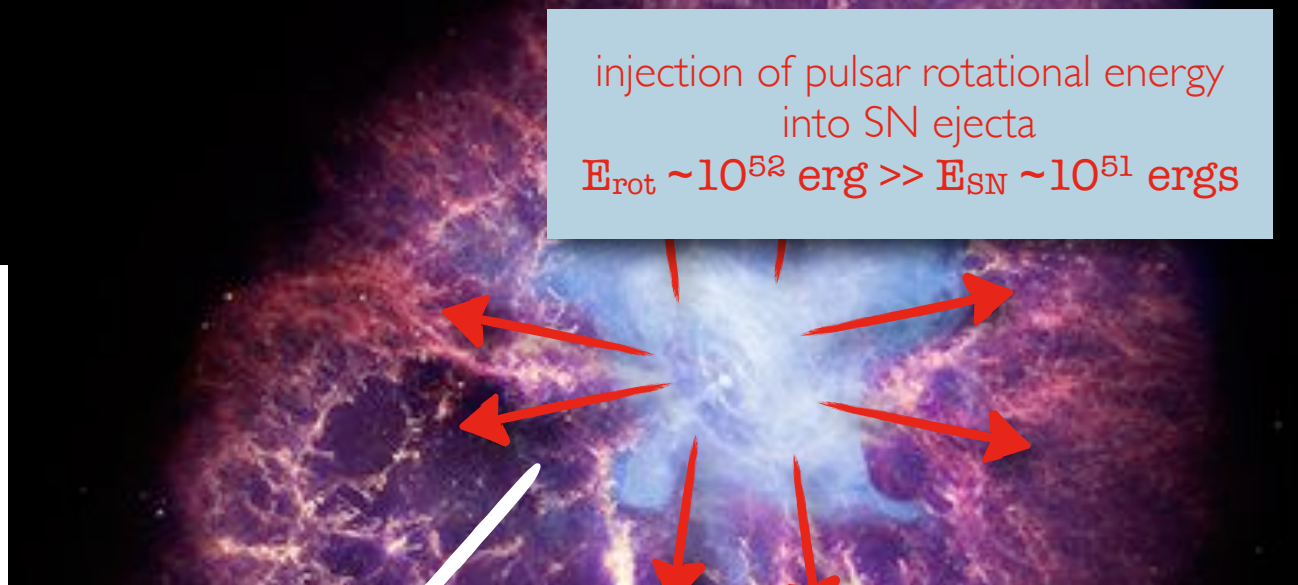
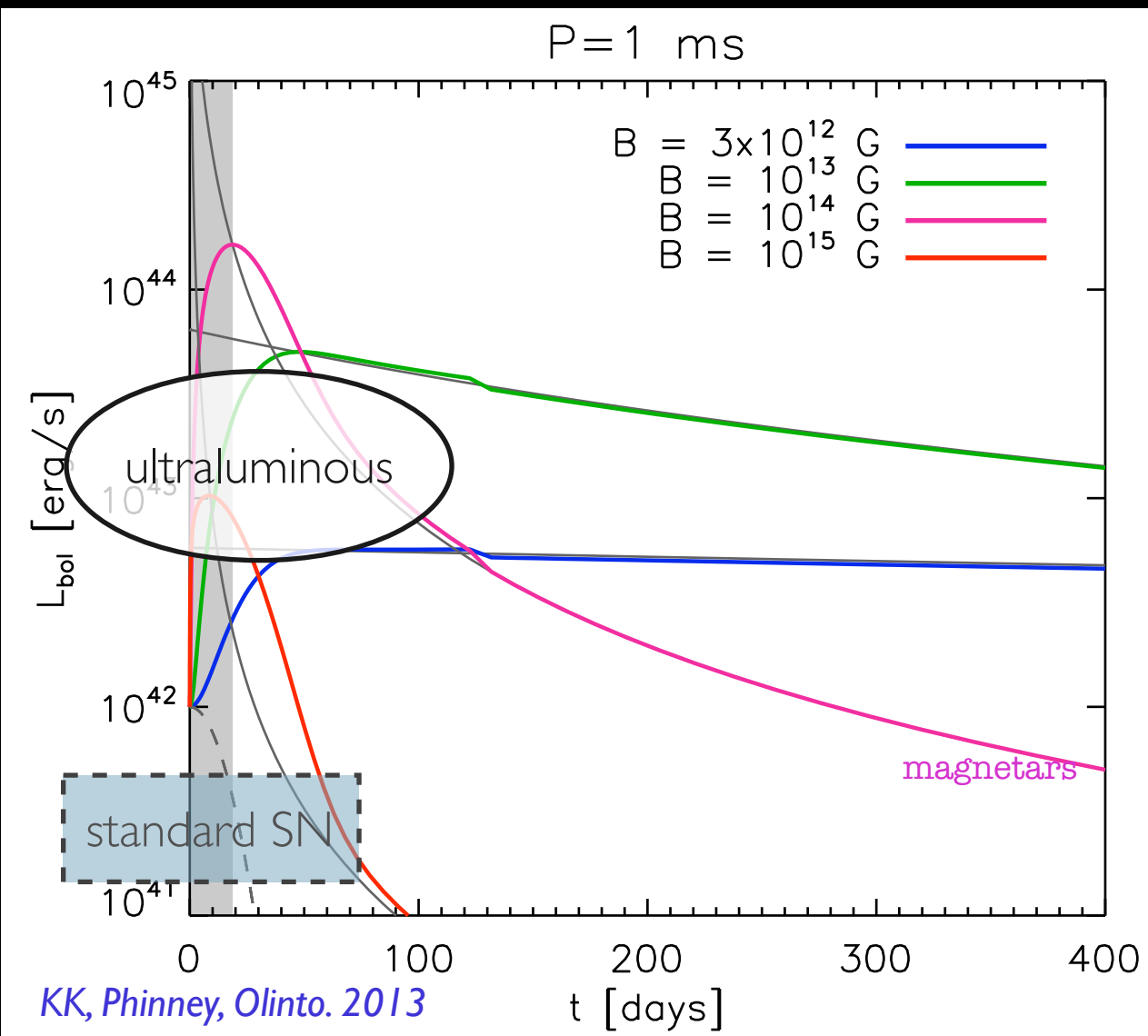


FIG. 7.— High-energy photon spectra of the early PWN embedded in the SN ejecta for $P_i = 2$ ms at $t = 10^{7.5}$ s ≈ 316 d. Different magnetic field strengths are considered. Detections with CTA are possible for $B_{\text{dip}} = 10^{13}$ G.

Murase et al. 2015

Superluminous supernovae due to central pulsar/magnetar

▶ superluminous supernovae lasting over a few days/months/years

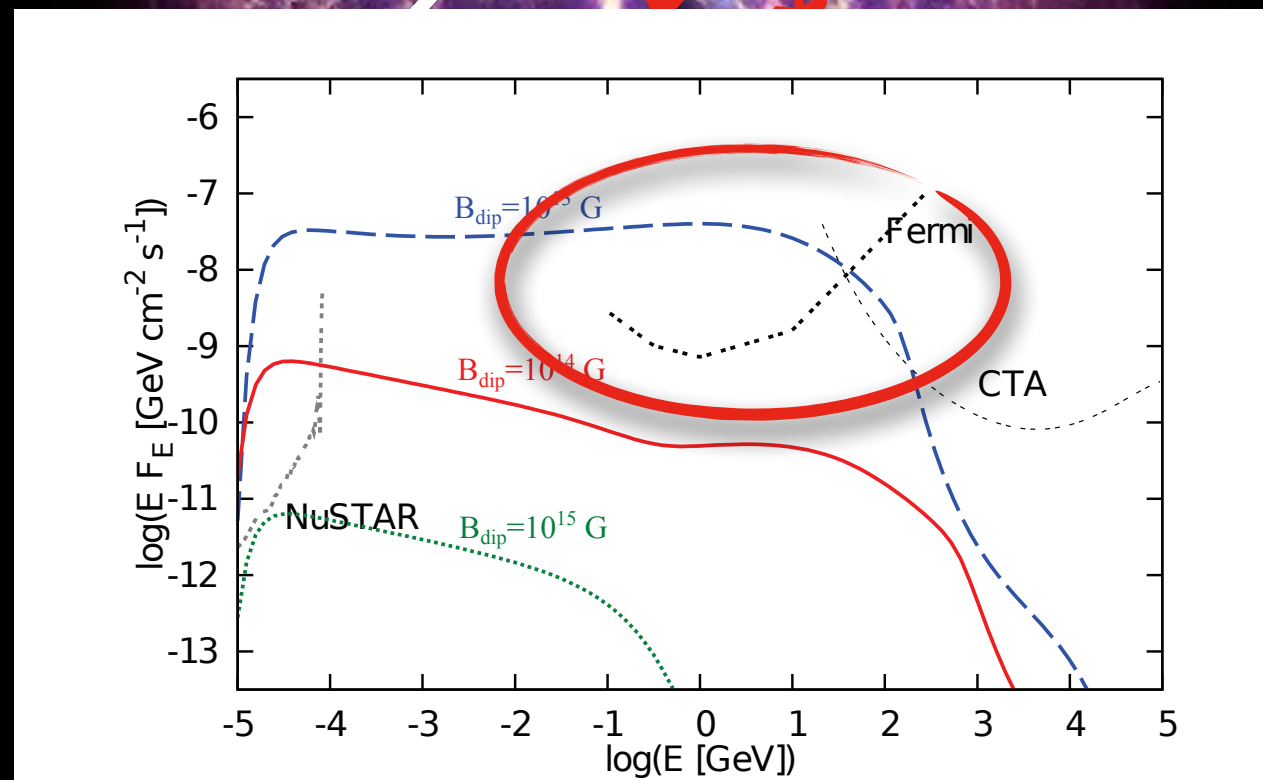
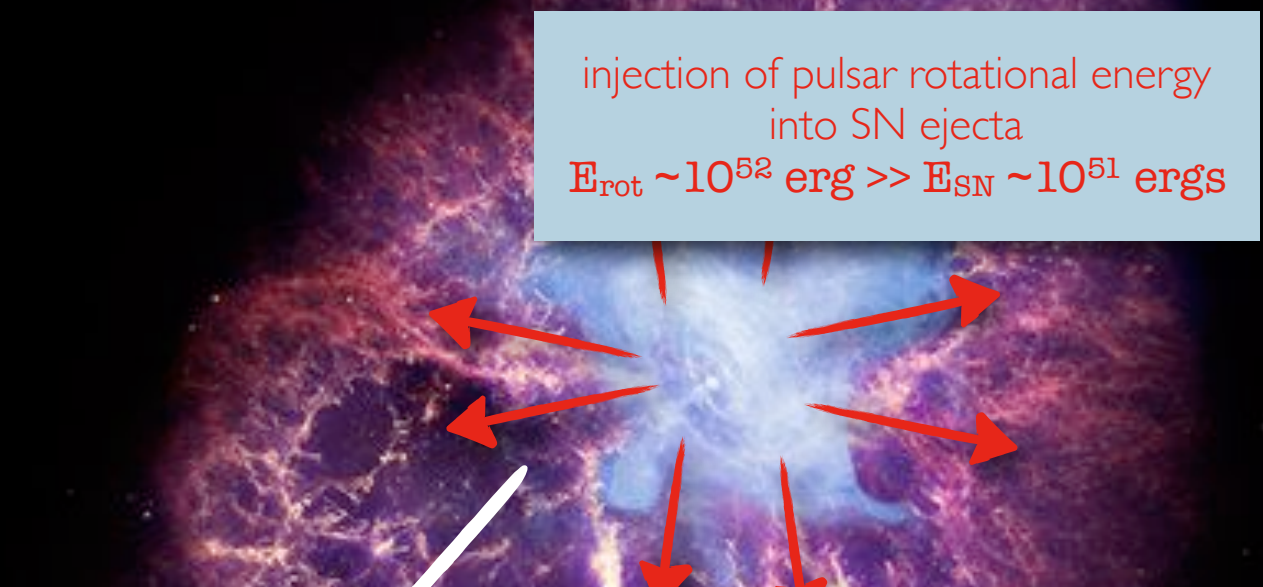
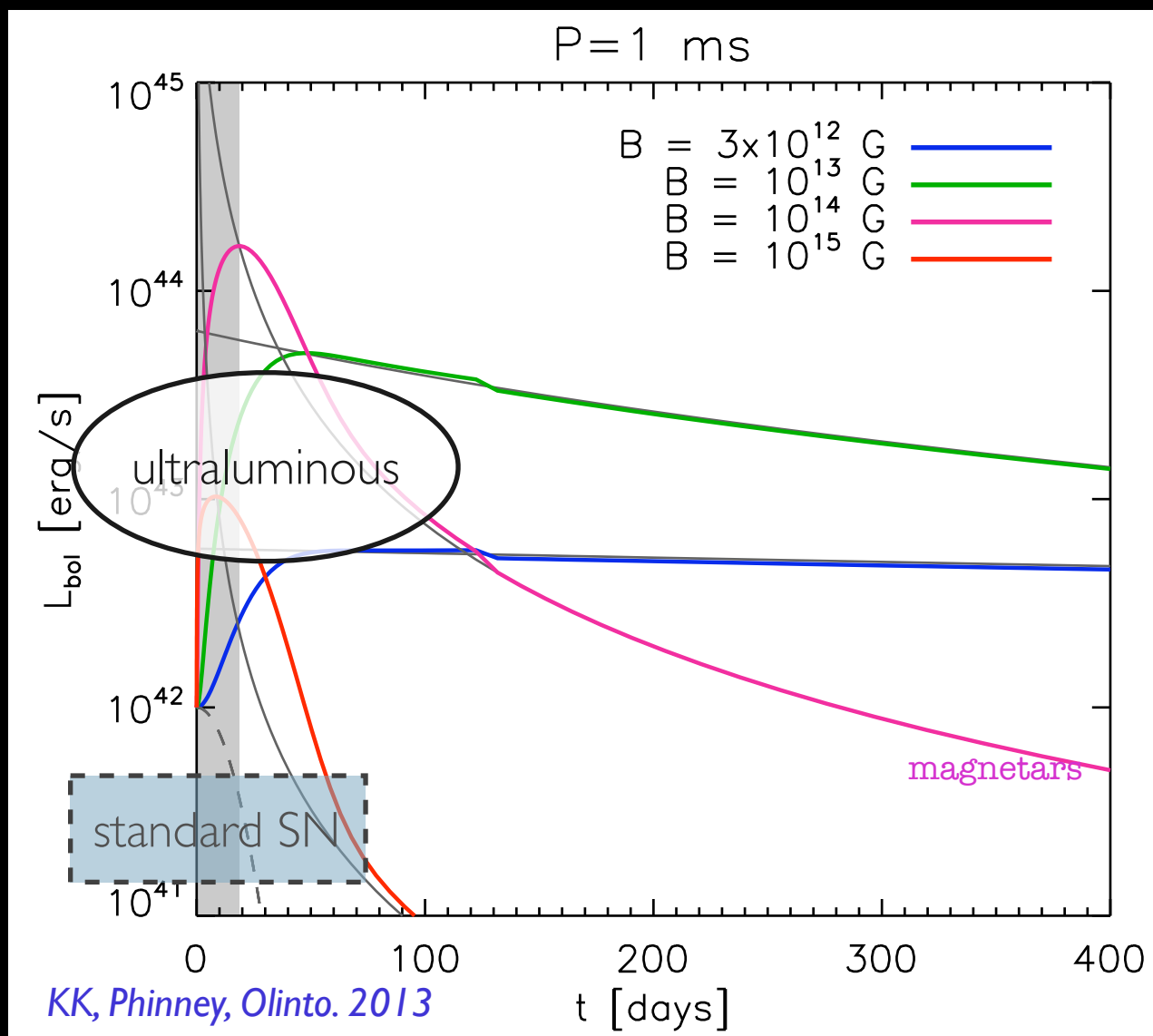


FIG. 7.— High-energy photon spectra of the early PWN embedded in the SN ejecta for $P_i = 2$ ms at $t = 10^{7.5}$ s \simeq 316 d. Different magnetic field strengths are considered. Detections with CTA are possible for $B_{\text{dip}} = 10^{13}$ G.

Murase et al. 2015

▶ systematic search with Fermi LAT @ location of SLSNe
 strong constraints on central object Renault-Tinacci, KK, et al. for the Fermi Coll., in prep. 8

sample of 39 SLSNe
Fermi Pass-8 data
3+1 and 7+1 bands in E: 0.6-600 GeV
4 different time windows

► Individual analysis

only source detected above 3-sigma level: SN2011ke
constraints on SLSNe luminosities: $< \sim 10^{44}$ erg/s

► Joint likelihood analysis (stacking)

Table 4: Luminosities from joint likelihood analysis measurements with the 7+1 energy band set and all sources.

| Time window | $\text{Sig}_{0.6-600.0 \text{ GeV}}$ σ units | $L_{0.6-10.2 \text{ GeV}}$ erg s ⁻¹ | $L_{0.6-600.0 \text{ GeV}}^{\text{sum}}$ erg s ⁻¹ | $\text{Sig}_{\text{E1-E2}}^{\text{best bnd}}$ σ units | E1 GeV | E2 GeV |
|---------------------------------------------------|--------------------------------------------------------|---------------------------------------------------|---------------------------------------------------------------------------------------------|-----------------------------------------------------------------|-----------|-----------|
| t_{peak} to $t_{\text{peak}} + 3$ months | 0.1 | $< 2.0 \times 10^{39}$ | 2.3×10^{38} $\begin{matrix} 2.0 \times 10^{39} \\ 1.8 \times 10^{38} \end{matrix}$ | 2.9 | 171.50 | 600.00 |
| t_{peak} to $t_{\text{peak}} + 6$ months | 0.0 | $< 1.6 \times 10^{39}$ | 2.5×10^{38} $\begin{matrix} 1.5 \times 10^{39} \\ 2.3 \times 10^{38} \end{matrix}$ | 2.8 | 171.50 | 600.00 |
| t_{peak} to $t_{\text{peak}} + 1$ year | 0.2 | $< 7.2 \times 10^{38}$ | $< 9.5 \times 10^{38}$ | 1.5 | 67.04 | 171.50 |
| t_{peak} to $t_{\text{peak}} + 2$ years | 0.0 | $< 6.6 \times 10^{38}$ | 1.2×10^{38} $\begin{matrix} 6.0 \times 10^{38} \\ 1.2 \times 10^{38} \end{matrix}$ | 3.8 | 67.04 | 171.50 |
| SN off-peak period | 1.6 | $< 3.5 \times 10^{38}$ | 9.6×10^{37} $\begin{matrix} 4.6 \times 10^{38} \\ 8.8 \times 10^{37} \end{matrix}$ | 2.2 | 26.21 | 67.04 |

sample of 39 SLSNe
Fermi Pass-8 data
3+1 and 7+1 bands in E: 0.6-600 GeV
4 different time windows

► Individual analysis

only source detected above 3-sigma level: SN2011ke
constraints on SLSNe luminosities: $< \sim 10^{44}$ erg/s

► Joint likelihood analysis (stacking)

Table 4: Luminosities from joint likelihood analysis measurements with the 7+1 energy band set and all sources.

| Time window | $\text{Sig}_{0.6-600.0 \text{ GeV}}$ σ units | $L_{0.6-10.2 \text{ GeV}}$ erg s ⁻¹ | $L_{0.6-600.0 \text{ GeV}}^{\text{sum}}$ erg s ⁻¹ | $\text{Sig}_{\text{E1-E2}}^{\text{best bnd}}$ σ units | E1 GeV | E2 GeV |
|---------------------------------------------------|--------------------------------------------------------|---------------------------------------------------|------------------------------------------------------------------------------------------------------------------------------------------------------------------------|-----------------------------------------------------------------|-----------|-----------|
| t_{peak} to $t_{\text{peak}} + 3$ months | 0.1 | $< 2.0 \times 10^{39}$ | 2.3×10^{38} 2.0×10^{39} 1.8×10^{38} | 2.9 | 171.50 | 600.00 |
| t_{peak} to $t_{\text{peak}} + 6$ months | 0.0 | $< 1.6 \times 10^{39}$ | 2.5×10^{38} 1.5×10^{39} 2.3×10^{38} | 2.8 | 171.50 | 600.00 |
| t_{peak} to $t_{\text{peak}} + 1$ year | 0.2 | $< 7.2 \times 10^{38}$ | $< 9.5 \times 10^{38}$ | 1.5 | 67.04 | 171.50 |
| t_{peak} to $t_{\text{peak}} + 2$ years | 0.0 | $< 6.6 \times 10^{38}$ | 1.2×10^{38} 6.0×10^{38} 1.2×10^{38} | 3.8 | 67.04 | 171.50 |
| SN off-peak period | 1.6 | $< 3.5 \times 10^{38}$ | 9.6×10^{37} 4.6×10^{38} 8.8×10^{37} | 2.2 | 26.21 | 67.04 |

sample of 39 SLSNe
Fermi Pass-8 data
3+1 and 7+1 bands in E: 0.6-600 GeV
4 different time windows

- ▶ Individual analysis
only source detected above 3-sigma level: SN2011ke
constraints on SLSNe luminosities: $< \sim 10^{44}$ erg/s
- ▶ Joint likelihood analysis (stacking)

▶ strong constraints on (P, B) of central object!

$$L_{\gamma, \epsilon} \sim \xi \beta_{ej} \eta_e \frac{L_{rot}}{4} \sim 6.0 \times 10^{42} \text{ erg s}^{-1} \xi P_{-3}^{-5} B_{13}^2 R_6^6 I_{45}^{1/2} M_{ej,5}^{-1/2}$$

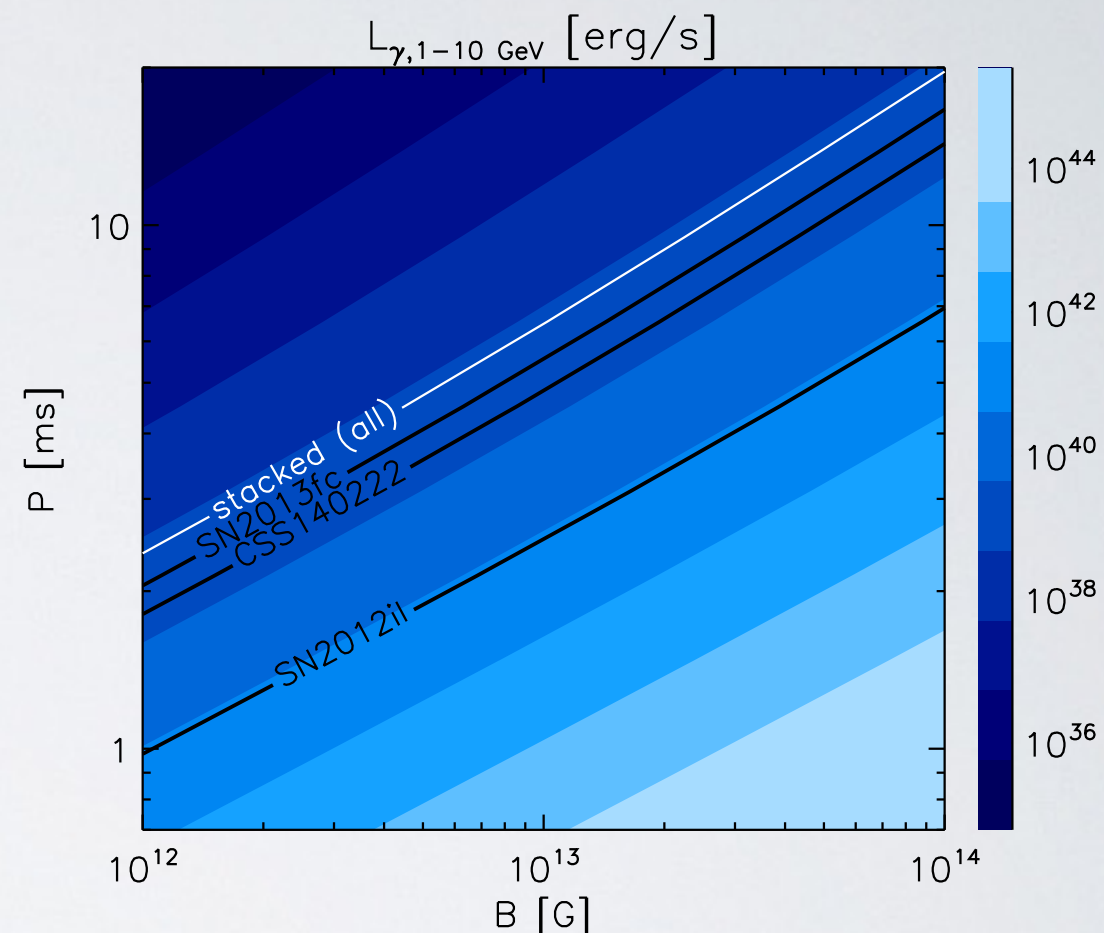


Table 4: Luminosities from joint likelihood analysis measurements with the 7+1 energy band set and all sources.

| Time window | $\text{Sig}_{0.6-600.0 \text{ GeV}}$ σ units | $L_{0.6-10.2 \text{ GeV}}$ erg s^{-1} | $L_{0.6-600.0 \text{ GeV}}^{\text{sum}}$ erg s^{-1} | $\text{Sig}_{\text{E1-E2}}^{\text{best bnd}}$ σ units | E1 GeV | E2 GeV |
|---------------------------------------------------|--------------------------------------------------------|---------------------------------------------------|-------------------------------------------------------------------|-----------------------------------------------------------------|-----------|-----------|
| t_{peak} to $t_{\text{peak}} + 3$ months | 0.1 | $< 2.0 \times 10^{39}$ | 2.3×10^{38} 2.0×10^{39} 1.8×10^{38} | 2.9 | 171.50 | 600.00 |
| t_{peak} to $t_{\text{peak}} + 6$ months | 0.0 | $< 1.6 \times 10^{39}$ | 2.5×10^{38} 1.5×10^{39} 2.3×10^{38} | 2.8 | 171.50 | 600.00 |
| t_{peak} to $t_{\text{peak}} + 1$ year | 0.2 | $< 7.2 \times 10^{38}$ | $< 9.5 \times 10^{38}$ | 1.5 | 67.04 | 171.50 |
| t_{peak} to $t_{\text{peak}} + 2$ years | 0.0 | $< 6.6 \times 10^{38}$ | 1.2×10^{38} 6.0×10^{38} 1.2×10^{38} | 3.8 | 67.04 | 171.50 |
| SN off-peak period | 1.6 | $< 3.5 \times 10^{38}$ | 9.6×10^{37} 4.6×10^{38} 8.8×10^{37} | 2.2 | 26.21 | 67.04 |

sample of 39 SLSNe
Fermi Pass-8 data
3+1 and 7+1 bands in E: 0.6-600 GeV
4 different time windows

- ▶ Individual analysis
only source detected above 3-sigma level: SN2011ke
constraints on SLSNe luminosities: $< \sim 10^{44}$ erg/s
- ▶ Joint likelihood analysis (stacking)

▶ strong constraints on (P, B) of central object!

$$L_{\gamma, \epsilon} \sim \xi \beta_{ej} \eta_e \frac{L_{rot}}{4} \sim 6.0 \times 10^{42} \text{ erg s}^{-1} \xi P_{-3}^{-5} B_{13}^2 R_6^6 I_{45}^{1/2} M_{ej,5}^{-1/2}$$

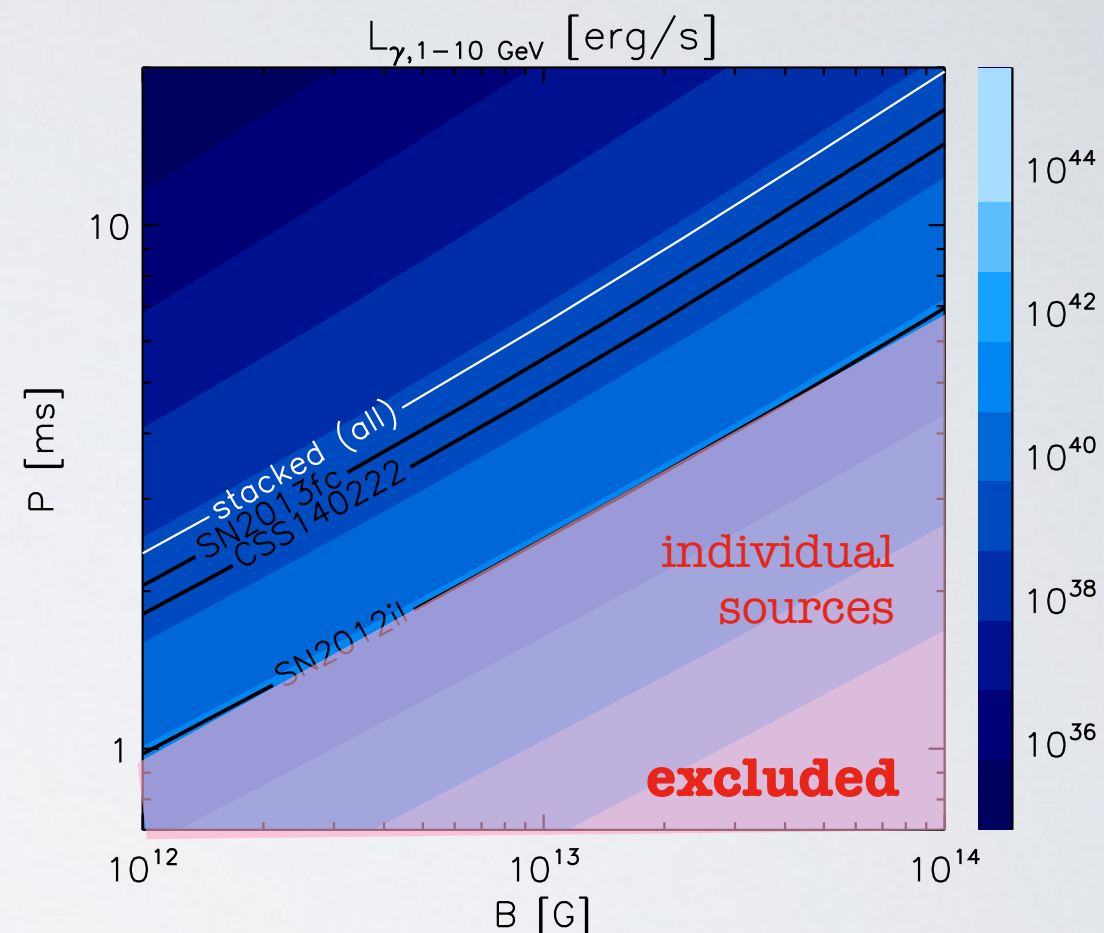


Table 4: Luminosities from joint likelihood analysis measurements with the 7+1 energy band set and all sources.

| Time window | $\text{Sig}_{0.6-600.0 \text{ GeV}}$ σ units | $L_{0.6-10.2 \text{ GeV}}$ erg s^{-1} | $L_{0.6-600.0 \text{ GeV}}^{\text{sum}}$ erg s^{-1} | $\text{Sig}_{\text{E1-E2}}^{\text{best bnd}}$ σ units | E1 GeV | E2 GeV |
|---------------------------------------------------|--------------------------------------------------------|---------------------------------------------------|-------------------------------------------------------------------|-----------------------------------------------------------------|-----------|-----------|
| t_{peak} to $t_{\text{peak}} + 3$ months | 0.1 | $< 2.0 \times 10^{39}$ | 2.3×10^{38} 2.0×10^{39} 1.8×10^{38} | 2.9 | 171.50 | 600.00 |
| t_{peak} to $t_{\text{peak}} + 6$ months | 0.0 | $< 1.6 \times 10^{39}$ | 2.5×10^{38} 1.5×10^{39} 2.3×10^{38} | 2.8 | 171.50 | 600.00 |
| t_{peak} to $t_{\text{peak}} + 1$ year | 0.2 | $< 7.2 \times 10^{38}$ | $< 9.5 \times 10^{38}$ | 1.5 | 67.04 | 171.50 |
| t_{peak} to $t_{\text{peak}} + 2$ years | 0.0 | $< 6.6 \times 10^{38}$ | 1.2×10^{38} 6.0×10^{38} 1.2×10^{38} | 3.8 | 67.04 | 171.50 |
| SN off-peak period | 1.6 | $< 3.5 \times 10^{38}$ | 9.6×10^{37} 4.6×10^{38} 8.8×10^{37} | 2.2 | 26.21 | 67.04 |

sample of 39 SLSNe
Fermi Pass-8 data
3+1 and 7+1 bands in E: 0.6-600 GeV
4 different time windows

- ▶ Individual analysis
only source detected above 3-sigma level: SN2011ke
constraints on SLSNe luminosities: $< \sim 10^{44}$ erg/s
- ▶ Joint likelihood analysis (stacking)

▶ strong constraints on (P, B) of central object!

$$L_{\gamma, \epsilon} \sim \xi \beta_{ej} \eta_e \frac{L_{rot}}{4} \sim 6.0 \times 10^{42} \text{ erg s}^{-1} \xi P_{-3}^{-5} B_{13}^2 R_6^6 I_{45}^{1/2} M_{ej,5}^{-1/2}$$

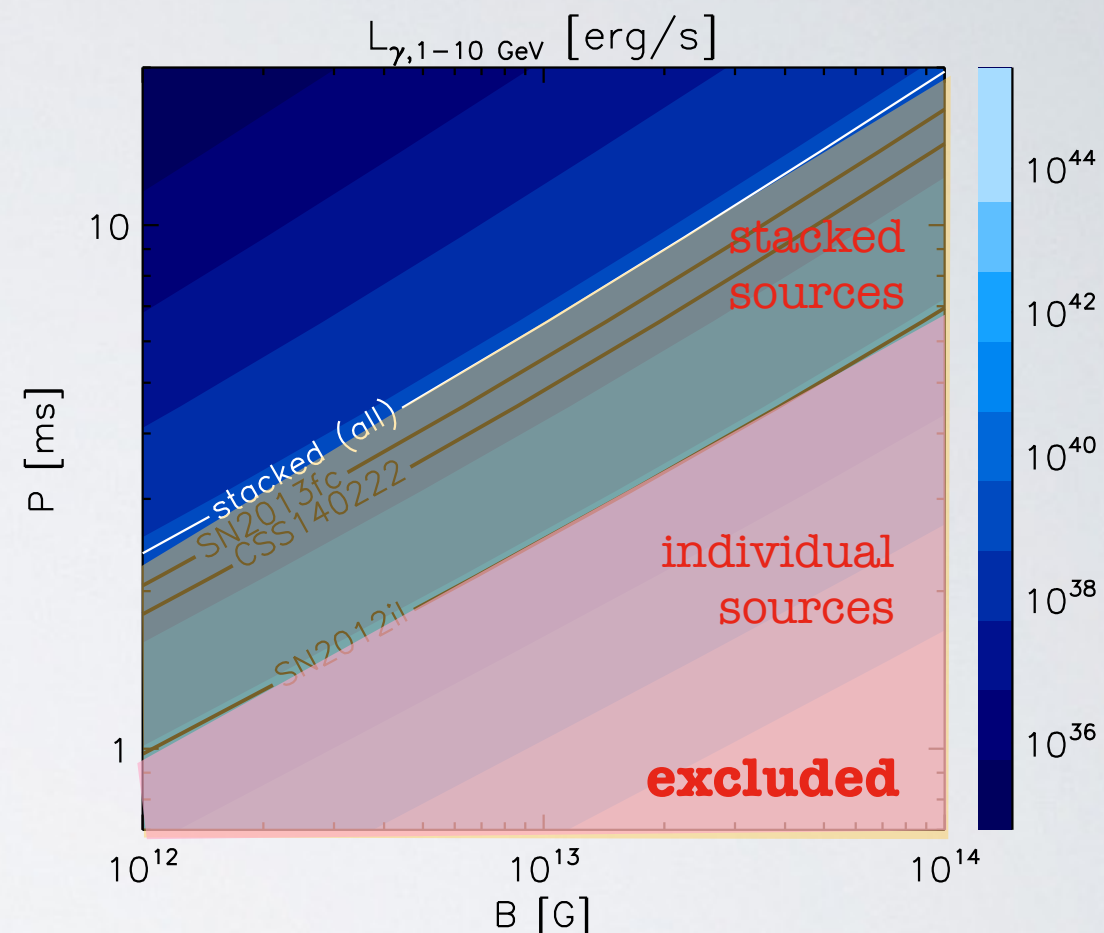


Table 4: Luminosities from joint likelihood analysis measurements with the 7+1 energy band set and all sources.

| Time window | $\text{Sig}_{0.6-600.0 \text{ GeV}}$ σ units | $L_{0.6-10.2 \text{ GeV}}$ erg s^{-1} | $L_{0.6-600.0 \text{ GeV}}^{\text{sum}}$ erg s^{-1} | $\text{Sig}_{\text{E1-E2}}^{\text{best bnd}}$ σ units | E1 GeV | E2 GeV |
|---------------------------------------------------|--------------------------------------------------------|---------------------------------------------------|-------------------------------------------------------------------|-----------------------------------------------------------------|-----------|-----------|
| t_{peak} to $t_{\text{peak}} + 3$ months | 0.1 | $< 2.0 \times 10^{39}$ | 2.3×10^{38} 2.0×10^{39} 1.8×10^{38} | 2.9 | 171.50 | 600.00 |
| t_{peak} to $t_{\text{peak}} + 6$ months | 0.0 | $< 1.6 \times 10^{39}$ | 2.5×10^{38} 1.5×10^{39} 2.3×10^{38} | 2.8 | 171.50 | 600.00 |
| t_{peak} to $t_{\text{peak}} + 1$ year | 0.2 | $< 7.2 \times 10^{38}$ | $< 9.5 \times 10^{38}$ | 1.5 | 67.04 | 171.50 |
| t_{peak} to $t_{\text{peak}} + 2$ years | 0.0 | $< 6.6 \times 10^{38}$ | 1.2×10^{38} 6.0×10^{38} 1.2×10^{38} | 3.8 | 67.04 | 171.50 |
| SN off-peak period | 1.6 | $< 3.5 \times 10^{38}$ | 9.6×10^{37} 4.6×10^{38} 8.8×10^{37} | 2.2 | 26.21 | 67.04 |

$$E_{\text{UHECR}} \gtrsim 3.2 \times 10^{53} \text{ erg} \left(\frac{\rho_0}{1 \text{ Gpc}^{-3} \text{ yr}^{-1}} \right)^{-1}$$

learnt from GW150914

► comfortable energetics:

- $E_{\text{GW}} = 3.0 + 0.5 M_{\text{sun}} c^2 \sim 5.4 \times 10^{54} \text{ erg}$ per source
- population rate $\rho_{\text{BH}} \sim 2 - 400 \text{ Gpc}^{-3} \text{ yr}^{-1}$
- **efficiency < 3%** required in UHECRs per event per unit of GW energy release

► heavy composition possible:

- iron-enriched residual debris around merging BHs

► luminosity extracted via Blandford-Znajek mechanism

$$L_{\text{BZ}} = \frac{(GM)^3 B^2}{c^5 R} \sim 3.2 \times 10^{46} \text{ erg s}^{-1} M_{100}^3 B_{11}^2 \frac{R_S}{R}$$

$$R_S = 2GM/c^2 \sim 3.0 \times 10^7 M_{100} \text{ cm}$$

$$E_{\text{UHECR}} \gtrsim 3.2 \times 10^{53} \text{ erg} \left(\frac{\rho_0}{1 \text{ Gpc}^{-3} \text{ yr}^{-1}} \right)^{-1}$$

learnt from GW150914

► comfortable energetics:

- $E_{\text{GW}} = 3.0 + 0.5 M_{\text{sun}} c^2 \sim 5.4 \times 10^{54} \text{ erg}$ per source
- population rate $\rho_{\text{BH}} \sim 2 - 400 \text{ Gpc}^{-3} \text{ yr}^{-1}$
- **efficiency < 3%** required in UHECRs per event per unit of GW energy release

► heavy composition possible:

- iron-enriched residual debris around merging BHs

► luminosity extracted via Blandford-Znajek mechanism

$$L_{\text{BZ}} = \frac{(GM)^3 B^2}{c^5 R} \sim 3.2 \times 10^{46} \text{ erg s}^{-1} M_{100}^3 B_{11}^2 \frac{R_S}{R}$$

$$R_S = 2GM/c^2 \sim 3.0 \times 10^7 M_{100} \text{ cm}$$

$$E_{\text{UHECR}} \gtrsim 3.2 \times 10^{53} \text{ erg} \left(\frac{\rho_0}{1 \text{ Gpc}^{-3} \text{ yr}^{-1}} \right)^{-1}$$

learnt from GW150914

► comfortable energetics:

- $E_{\text{GW}} = 3.0 + 0.5 M_{\text{sun}} c^2 \sim 5.4 \times 10^{54} \text{ erg}$ per source
- population rate $\rho_{\text{BH}} \sim 2 - 400 \text{ Gpc}^{-3} \text{ yr}^{-1}$
- **efficiency < 3%** required in UHECRs per event per unit of GW energy release

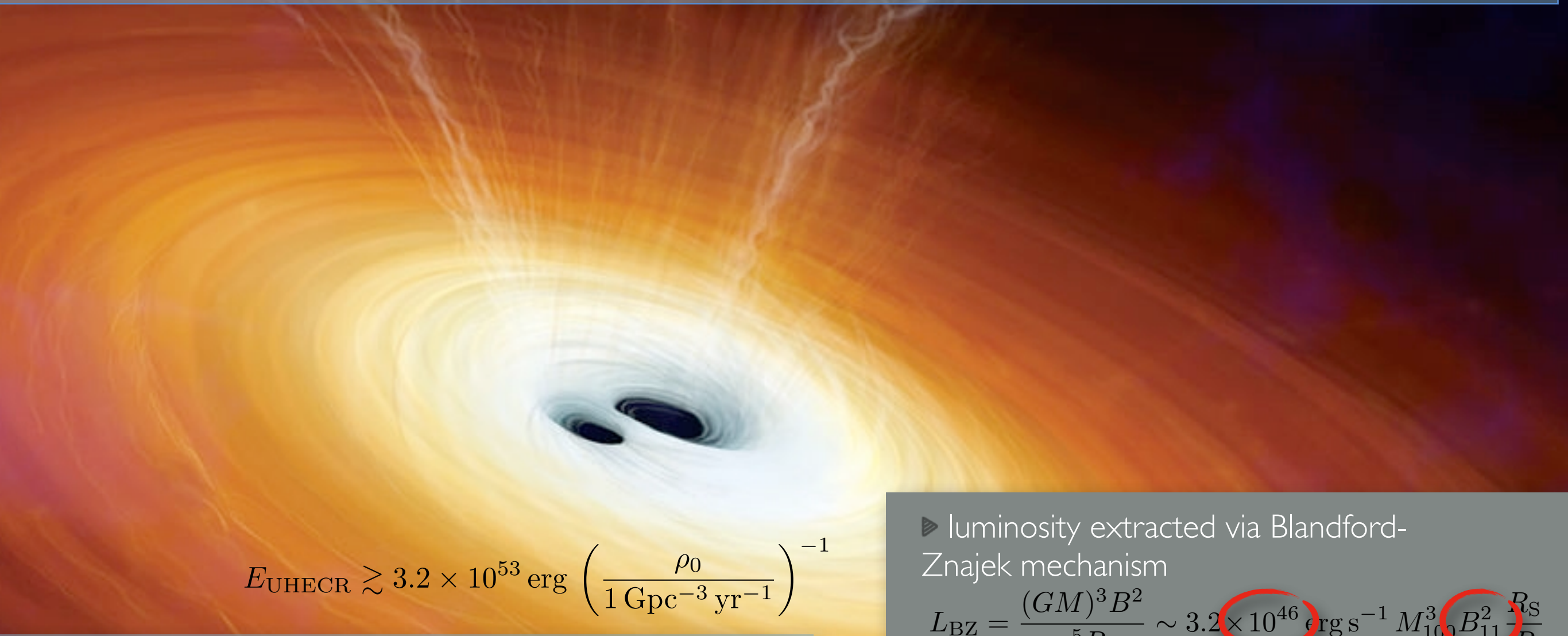
► heavy composition possible:

- iron-enriched residual debris around merging BHs

► luminosity extracted via Blandford-Znajek mechanism

$$L_{\text{BZ}} = \frac{(GM)^3 B^2}{c^5 R} \sim 3.2 \times 10^{46} \text{ erg s}^{-1} M_{100}^3 B_{11}^2 \frac{R_S}{R}$$

$$R_S = 2GM/c^2 \sim 3.0 \times 10^7 M_{100} \text{ cm}$$



$$E_{\text{UHECR}} \gtrsim 3.2 \times 10^{53} \text{ erg} \left(\frac{\rho_0}{1 \text{ Gpc}^{-3} \text{ yr}^{-1}} \right)^{-1}$$

learnt from GW150914

► comfortable energetics:

- $E_{\text{GW}} = 3.0 + 0.5 M_{\text{sun}} c^2 \sim 5.4 \times 10^{54} \text{ erg}$ per source
- population rate $\rho_{\text{BH}} \sim 2 - 400 \text{ Gpc}^{-3} \text{ yr}^{-1}$
- **efficiency < 3%** required in UHECRs per event per unit of GW energy release

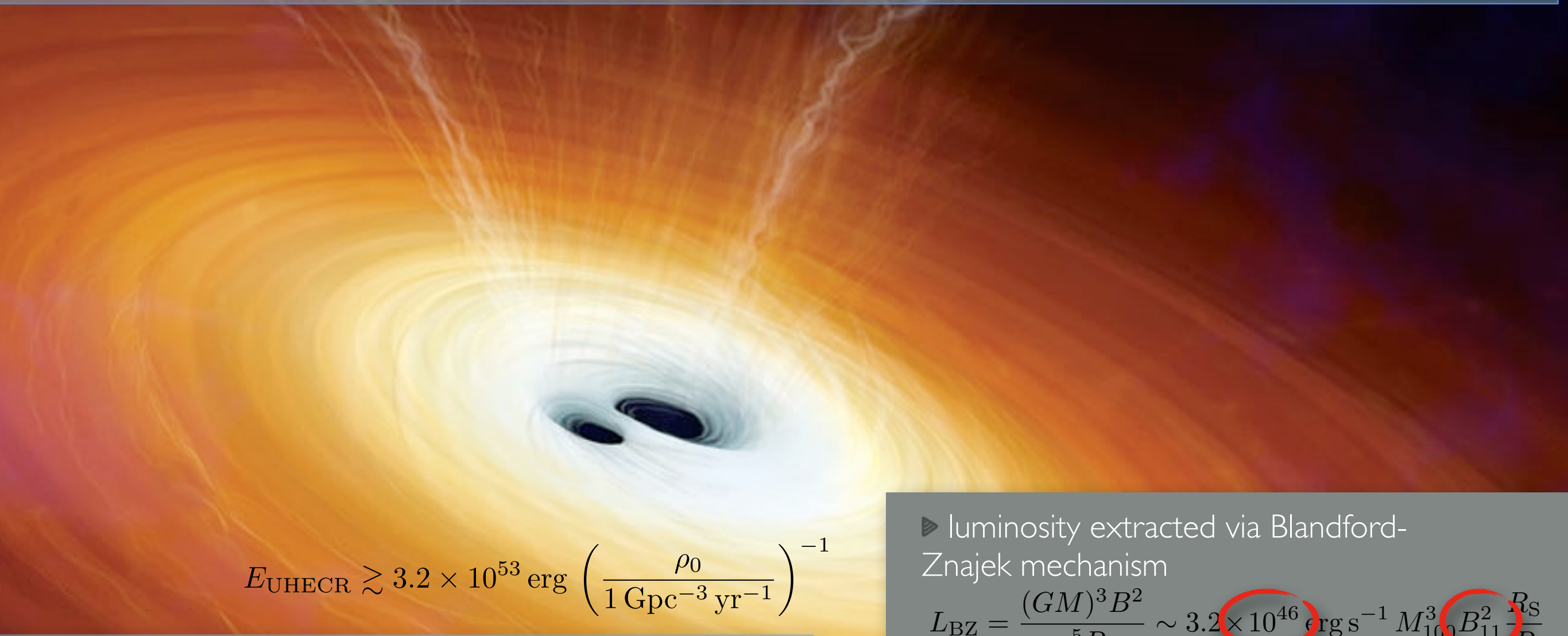
► heavy composition possible:

- iron-enriched residual debris around merging BHs

► luminosity extracted via Blandford-Znajek mechanism

$$L_{\text{BZ}} = \frac{(GM)^3 B^2}{c^5 R} \sim 3.2 \times 10^{46} \text{ erg s}^{-1} M_{100}^3 B_{11}^2 \frac{R_S}{R}$$

$$R_S = 2GM/c^2 \sim 3.0 \times 10^7 M_{100} \text{ cm}$$



$$E_{\text{UHECR}} \gtrsim 3.2 \times 10^{53} \text{ erg} \left(\frac{\rho_0}{1 \text{ Gpc}^{-3} \text{ yr}^{-1}} \right)^{-1}$$

learnt from GW150914

► comfortable energetics:

- $E_{\text{GW}} = 3.0 + 0.5 M_{\text{sun}} c^2 \sim 5.4 \times 10^{54} \text{ erg}$ per source
- population rate $\rho_{\text{BH}} \sim 2 - 400 \text{ Gpc}^{-3} \text{ yr}^{-1}$
- **efficiency < 3%** required in UHECRs per event per unit of GW energy release

► heavy composition possible:

- iron-enriched residual debris around merging BHs

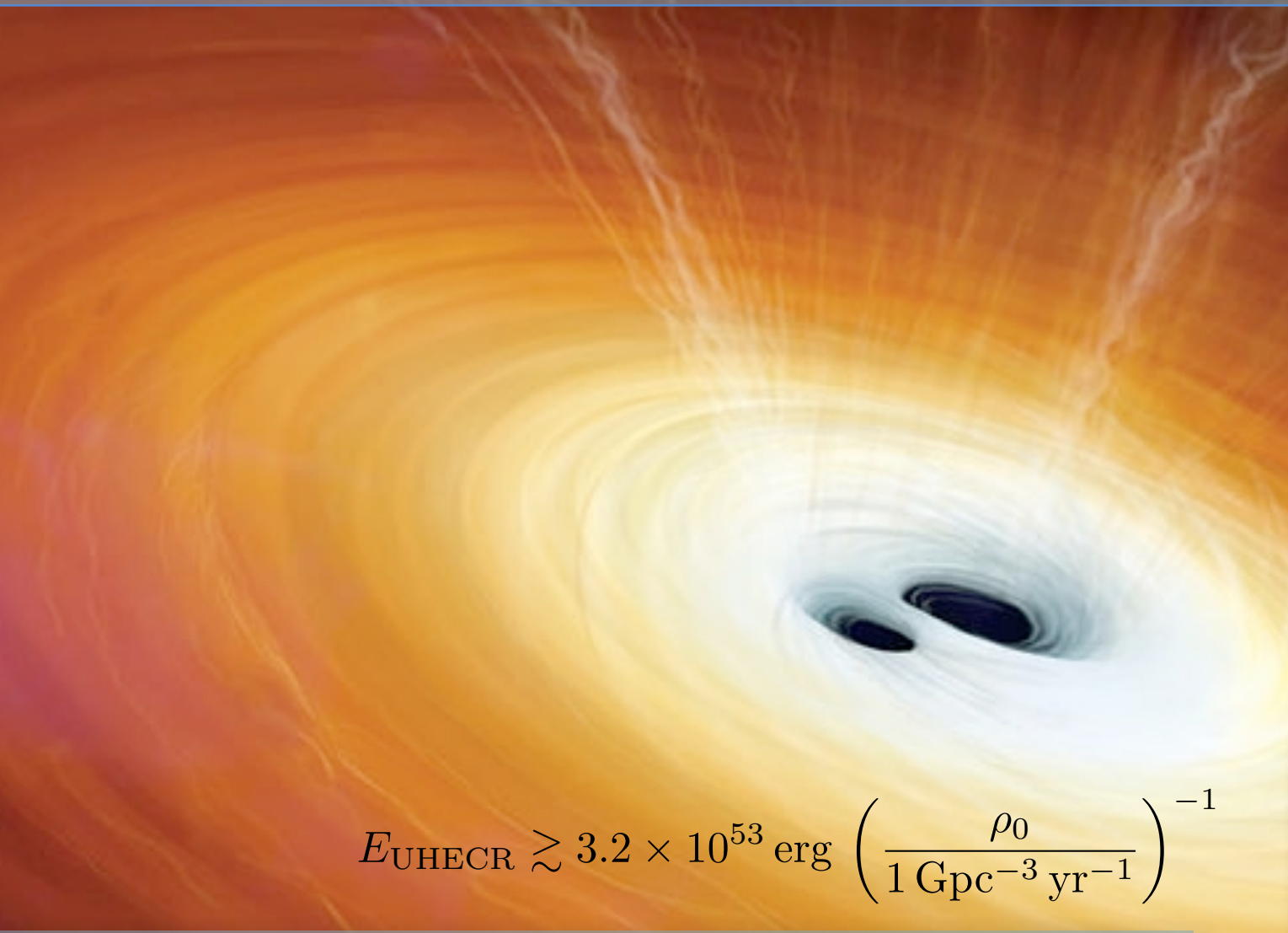
► luminosity extracted via Blandford-Znajek mechanism

$$L_{\text{BZ}} = \frac{(GM)^3 B^2}{c^5 R} \sim 3.2 \times 10^{46} \text{ erg s}^{-1} M_{100}^3 B_{11}^2 \frac{R_S}{R}$$

$$R_S = 2GM/c^2 \sim 3.0 \times 10^7 M_{100} \text{ cm}$$

► magnetic field strength via $\alpha\omega$ -dynamo

$$B \sim 10^{12} \text{ G} (P/300 \text{ ms})^{-1}$$



$$E_{\text{UHECR}} \gtrsim 3.2 \times 10^{53} \text{ erg} \left(\frac{\rho_0}{1 \text{ Gpc}^{-3} \text{ yr}^{-1}} \right)^{-1}$$

learnt from GW150914

comfortable energetics:

- ▶ $E_{\text{GW}} = 3.0 + 0.5 M_{\text{sun}} c^2 \sim 5.4 \times 10^{54} \text{ erg}$ per source
- ▶ population rate $\rho_{\text{BH}} \sim 2 - 400 \text{ Gpc}^{-3} \text{ yr}^{-1}$
- ▶ **efficiency < 3%** required in UHECRs per event per unit of GW energy release

heavy composition possible:

- ▶ iron-enriched residual debris around merging BHs

- ▶ luminosity extracted via Blandford-Znajek mechanism

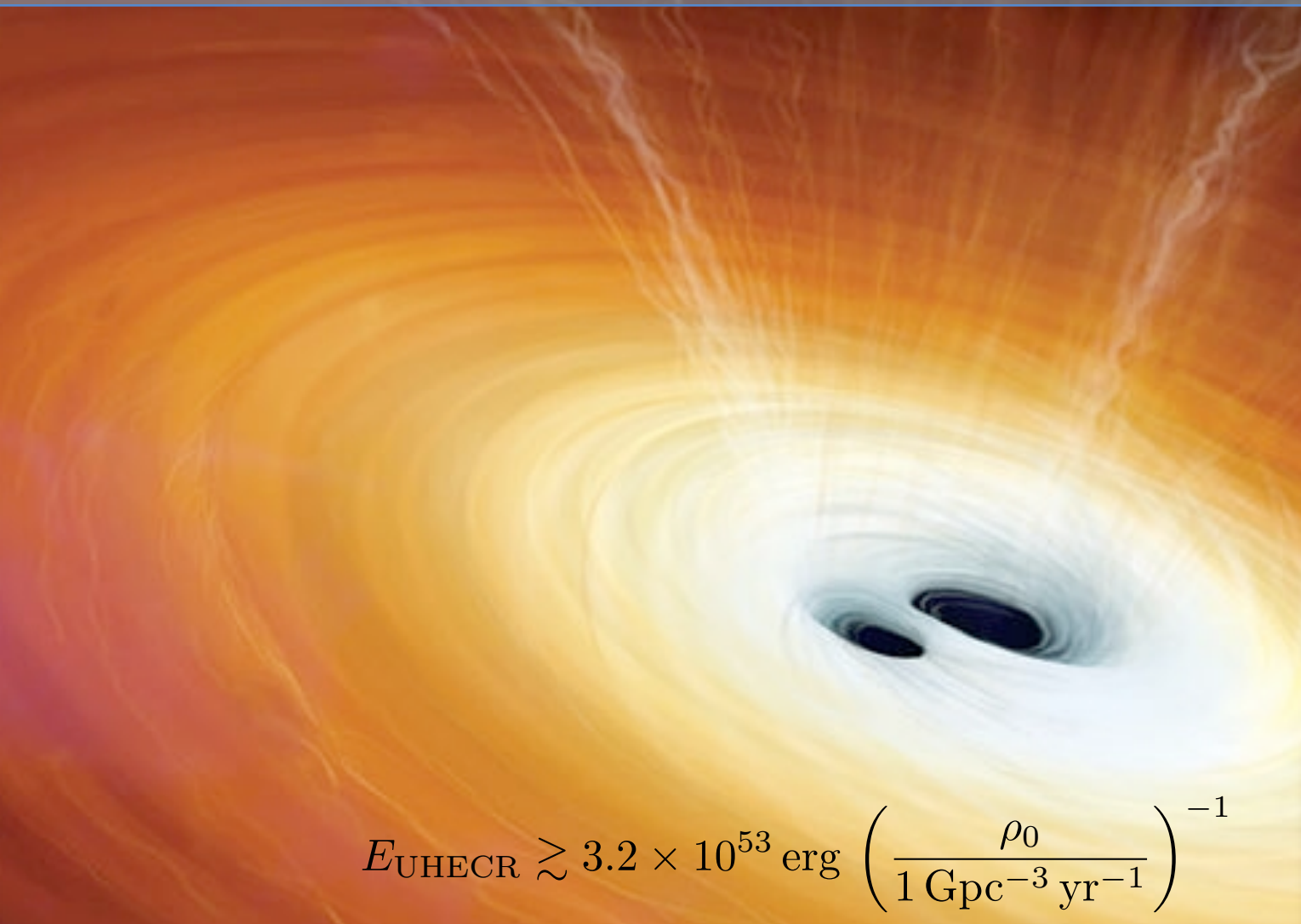
$$L_{\text{BZ}} = \frac{(GM)^3 B^2}{c^5 R} \sim 3.2 \times 10^{46} \text{ erg s}^{-1} M_{100}^3 B_{11}^2 \frac{R_S}{R}$$

$$R_S = 2GM/c^2 \sim 3.0 \times 10^7 M_{100} \text{ cm}$$

- ▶ magnetic field strength via $\alpha\omega$ -dynamo

$$B \sim 10^{12} \text{ G} (P/300 \text{ ms})^{-1}$$

- ▶ luminosity has to last for 7 hours to 2 months to reach E_{UHECR}



$$E_{\text{UHECR}} \gtrsim 3.2 \times 10^{53} \text{ erg} \left(\frac{\rho_0}{1 \text{ Gpc}^{-3} \text{ yr}^{-1}} \right)^{-1}$$

learnt from GW150914

comfortable energetics:

- ▶ $E_{\text{GW}} = 3.0 + 0.5 M_{\text{sun}} c^2 \sim 5.4 \times 10^{54} \text{ erg}$ per source
- ▶ population rate $\rho_{\text{BH}} \sim 2 - 400 \text{ Gpc}^{-3} \text{ yr}^{-1}$
- ▶ **efficiency < 3%** required in UHECRs per event per unit of GW energy release

heavy composition possible:

- ▶ iron-enriched residual debris around merging BHs

- ▶ luminosity extracted via Blandford-Znajek mechanism

$$L_{\text{BZ}} = \frac{(GM)^3 B^2}{c^5 R} \sim 3.2 \times 10^{46} \text{ erg s}^{-1} M_{100}^3 B_{11}^2 \frac{R_S}{R}$$

$$R_S = 2GM/c^2 \sim 3.0 \times 10^7 M_{100} \text{ cm}$$

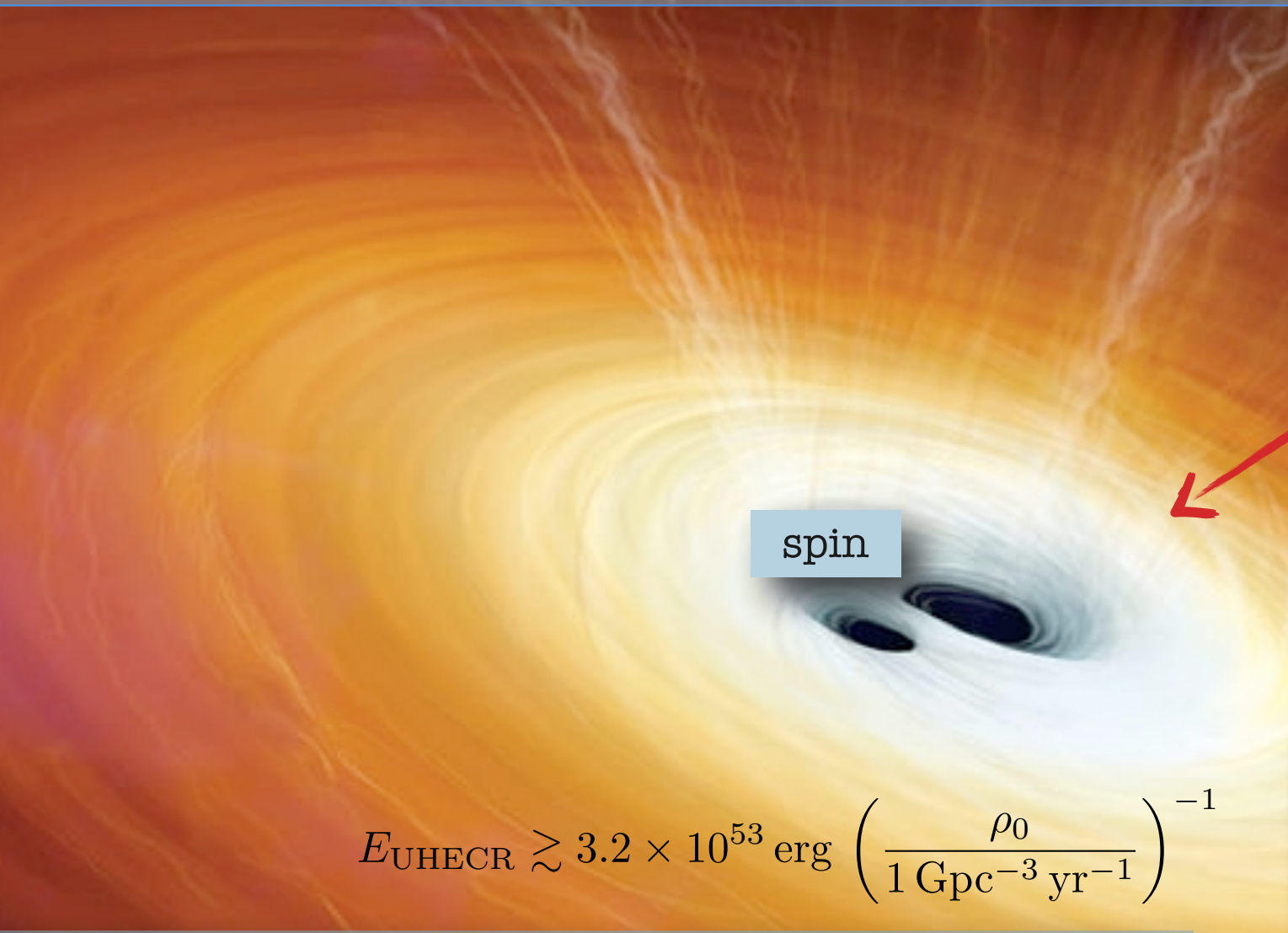
- ▶ magnetic field strength via $\alpha\omega$ -dynamo

$$B \sim 10^{12} \text{ G} (P/300 \text{ ms})^{-1}$$

- ▶ luminosity has to last for 7 hours to 2 months to reach E_{UHECR}

- ▶ BZ timescale (as long as BH accretes after merger - sourced by debris)

$$t_{\text{BZ}} = Mc^2/L_{\text{BZ}} \sim 22 M_{100} B_{11}^{-2} (R_S/R)^2 \text{ yr}$$



- ▶ accretion to source BZ long enough,
- ▶ disk to anchor fields and do $\alpha\omega$ -dynamo to generate strong magnetic field

debris

tidal disruption of asteroids or planets

spin

$$E_{\text{UHECR}} \gtrsim 3.2 \times 10^{53} \text{ erg} \left(\frac{\rho_0}{1 \text{ Gpc}^{-3} \text{ yr}^{-1}} \right)^{-1}$$

learnt from GW150914

▶ comfortable energetics:

- ▶ $E_{\text{GW}} = 3.0 \pm 0.5 M_{\text{sun}} c^2 \sim 5.4 \times 10^{54} \text{ erg}$ per source
- ▶ population rate $\rho_{\text{BH}} \sim 2 - 400 \text{ Gpc}^{-3} \text{ yr}^{-1}$
- ▶ **efficiency < 3%** required in UHECRs per event per unit of GW energy release

▶ heavy composition possible:

- ▶ iron-enriched residual debris around merging BHs

- ▶ luminosity extracted via Blandford-Znajek mechanism

$$L_{\text{BZ}} = \frac{(GM)^3 B^2}{c^5 R} \sim 3.2 \times 10^{46} \text{ erg s}^{-1} M_{100}^3 B_{11}^2 \frac{R_S}{R}$$

$$R_S = 2GM/c^2 \sim 3.0 \times 10^7 M_{100} \text{ cm}$$

- ▶ magnetic field strength via $\alpha\omega$ -dynamo

$$B \sim 10^{12} \text{ G} (P/300 \text{ ms})^{-1}$$

- ▶ luminosity has to last for 7 hours to 2 months to reach E_{UHECR}

- ▶ BZ timescale (as long as BH accretes after merger - sourced by debris)

$$t_{\text{BZ}} = Mc^2/L_{\text{BZ}} \sim 22 M_{100} B_{11}^{-2} (R_S/R)^2 \text{ yr}$$

- ▶ **neutrinos**: similar predictions as for GRBs
or as for low mass ejecta (AIC type) + pulsar, as in *Piro et al. (2016)*
Compatible with non observation of associated neutrinos with IceCube and ANTARES

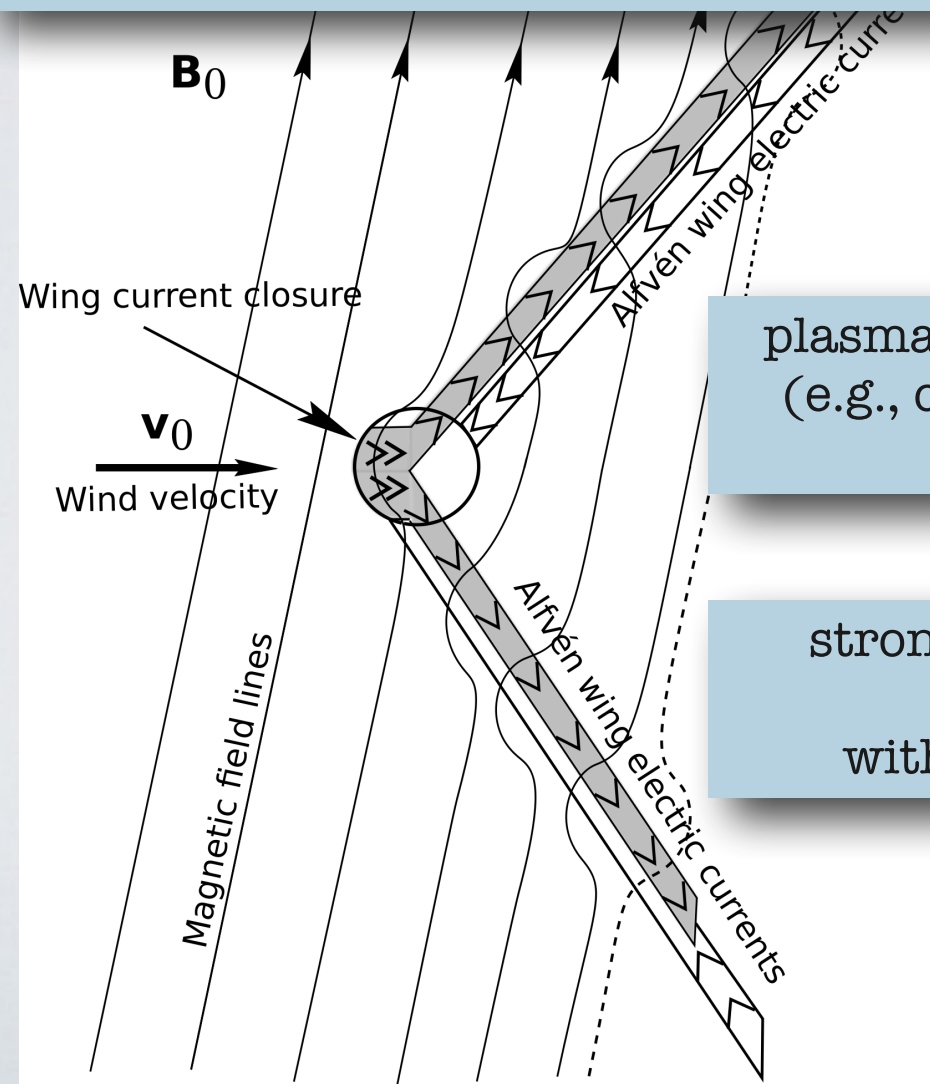
- ▶ **neutrinos:** similar predictions as for GRBs
or as for low mass ejecta (AIC type) + pulsar, as in *Piro et al. (2016)*
Compatible with non observation of associated neutrinos with IceCube and ANTARES

▶ Fast Radio Bursts!

(very bright radio bursts, routinely detected, of unknown cosmological origin)

Debris/bodies required around merging black holes/final black hole → model of *Mottez & Zarka (2013)*

a body immersed in a highly magnetized outflow
generates 2 stationary Alfvén wings



NB: asteroids and planets can orbit at close distance from the central object without being evaporated/destroyed (Mie Theory)

KK, Mottez, Voisin, Heyvaerts 2016

plasma instabilities in Alfvén wings
(e.g., cyclotron maser instability):
radio emission

strongly beamed radio emission
@ 10 MHz- 10^3 GHz
with high flux (Jansky level)

Mottez & Zarka 2013

How to look for multi-messenger transient signals

▶ UHECRs



a hotspot?
TA hotspot?

hotspot could be signature of Galactic transient source occurred 10^{3-4} yrs ago
or extragalactic transient at few 10s Mpc 10^5 yrs ago

Fang et al. 2015

Fargion 2015

H. He and D. Ryu's talks *He et al. 2016*

Renault-Tinacci, KK, Olinto in prep.

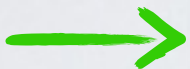
▶ neutrinos



identify best detector
characteristics for
neutrino astronomy

next slide

▶ photons



boom in time-domain astronomy
(PTF, Pan-STARRS, LSST, ...)
gamma-rays: Fermi, HESS, CTA

▶ GW

▶ real-time analysis (alerts/follow-up)

How to look for multi-messenger transient signals

▶ UHECRs



a hotspot?
TA hotspot?

hotspot could be signature of Galactic transient source occurred 10^{3-4} yrs ago or extragalactic transient at few 10s Mpc 10^5 yrs ago

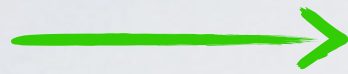
Fang et al. 2015

Fargion 2015

H. He and D. Ryu's talks He et al. 2016

Renault-Tinacci, KK, Olinto in prep.

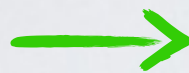
▶ neutrinos



identify best detector characteristics for neutrino astronomy

next slide

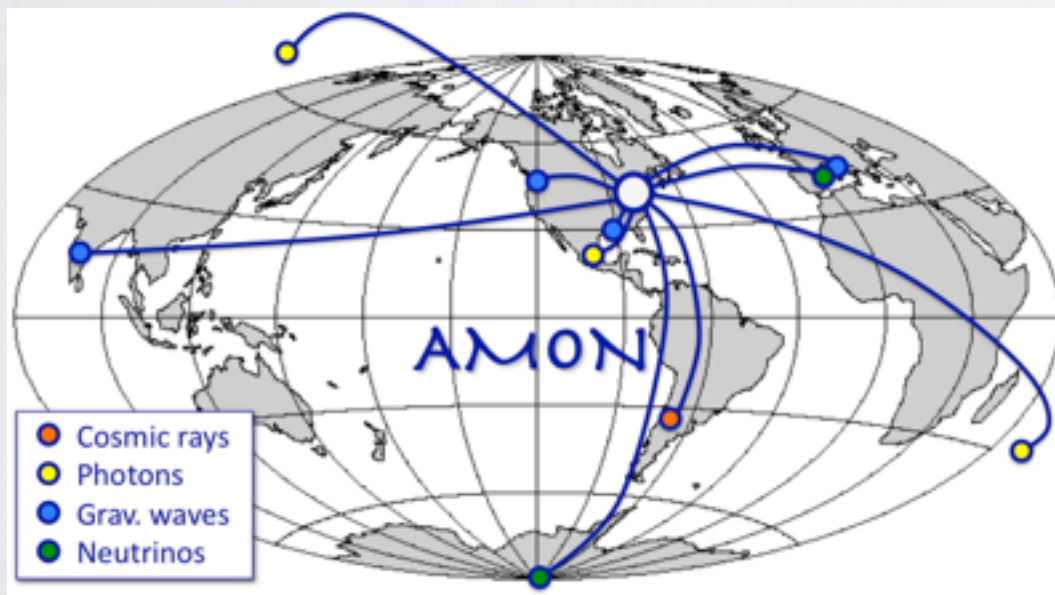
▶ photons



boom in time-domain astronomy (PTF, Pan-STARRS, LSST, ...) gamma-rays: Fermi, HESS, CTA

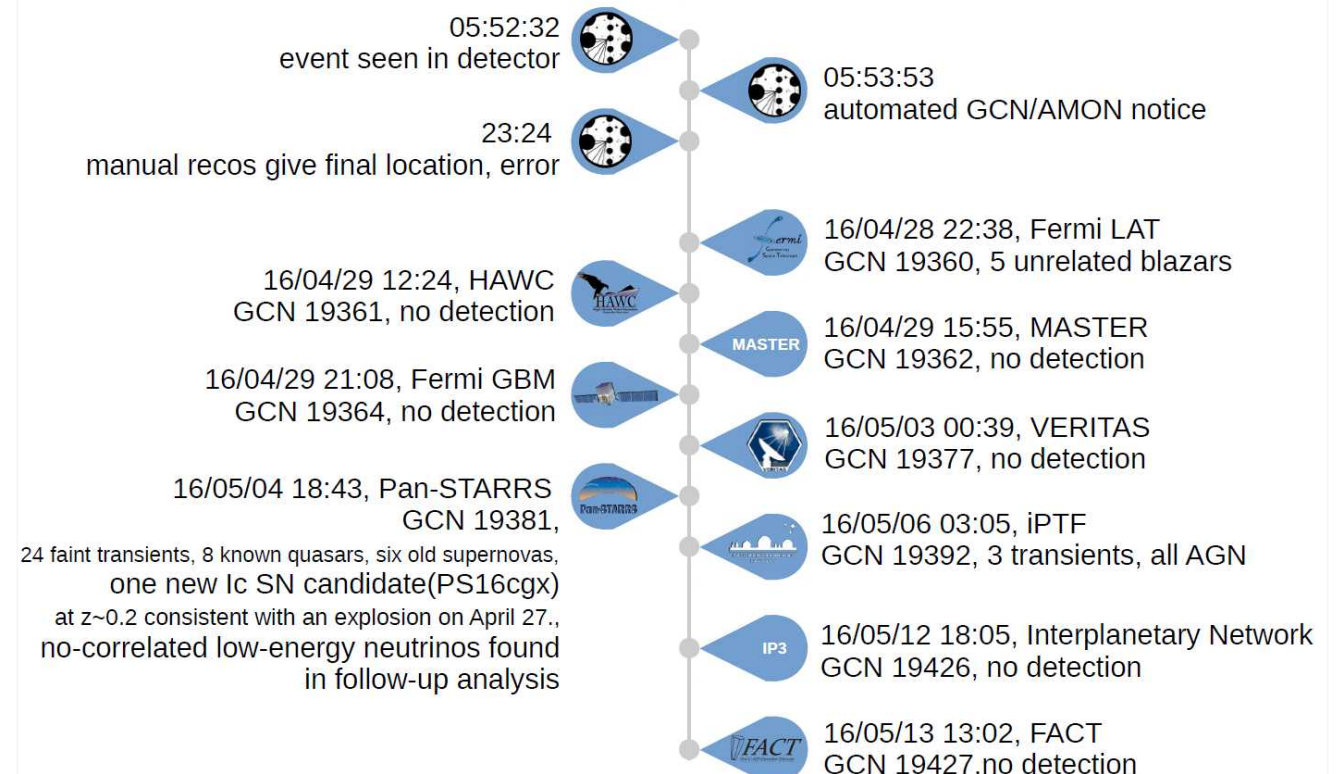
▶ GW

▶ real-time analysis (alerts/follow-up)



Astrophysical Multimessenger Observatory Network

Example: HESE-160427A , on April 27 2016



Naoko Kurahashi Neilson, Drexel University

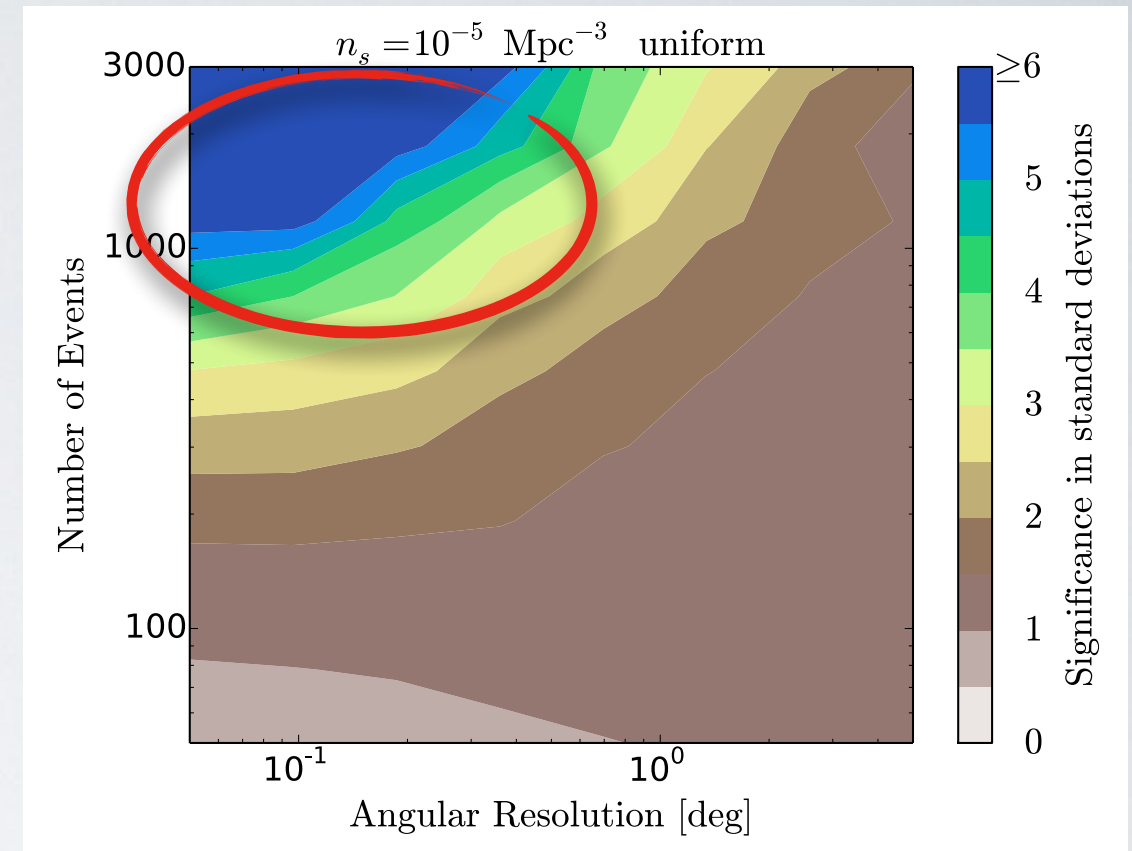
25

How to search for multi-messenger transient signals: neutrino sources?

- ▶ no deflection, no time delay, ideal?
- ▶ BUT: no horizon —> possible to spot source on top of background?

e.g., difficult to identify sources for IceCube neutrinos...

>1000 events and <1 deg. angular resolution required

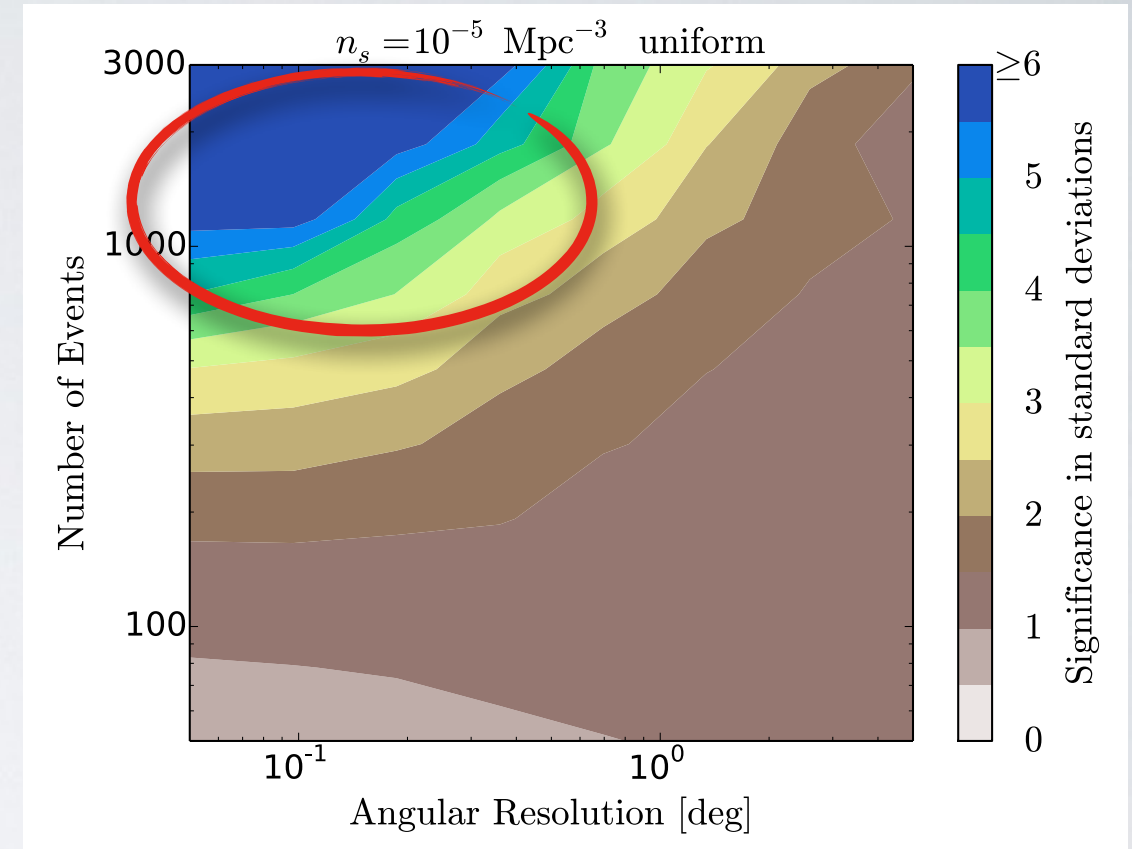


Fang, KK, Murase, Miller, Oikonomou, submitted

How to search for multi-messenger transient signals: neutrino sources?

- ▶ no deflection, no time delay, ideal?
 - ▶ BUT: no horizon —> possible to spot source on top of background?
- e.g., difficult to identify sources for IceCube neutrinos...

>1000 events and <1 deg. angular resolution required



Fang, KK, Murase, Miller, Oikonomou, submitted



Giant Radio Array for Neutrino Detection

200'000 radio antennas over 200'000 km²
 >1000 events in 10 yrs ($E > 10^{17}$ eV)
 < 0.3 deg. angular resolution

- ▶ ICRC 2015: [arXiv:1508.01919](https://arxiv.org/abs/1508.01919)

